APPLICATION OF THE ELECTRICAL RESISTIVITY AND GROUND PENETRATION RADAR METHODS IN LITHOSTRATIGRAPHY CHARACTERISATION OF THE KYEREYIASE CLAY DEPOSIT SITE, IN THE ATWIMA NWABIAGYA SOUTH DISTRICT OF THE ASHANTI REGION, GHANA

BY

AMFOH FELIX (BSC. GEOLOGICAL ENGINEERING)

THESIS SUBMITTED TO THE DEPARTMENT OF PHYSICS, FACULTY OF PHYSICAL AND COMPUTATIONAL SCIENCES, KWAME NKRUMAH UNIVERSITY OF SCIENCE AND TECHNOLOGY, IN PARTIAL FULFILLMENT OF THE REQUIREMENT FOR THE DEGREE OF

MASTER OF PHILOSOPHY (GEOPHYSICS) (COLLEGE OF SCIENCE)

SUPERVISOR: DR. D.D. WEMEGAH

©DEPARTMENT OF PHYSICS

JUNE, 2019

DECLARATION

I hereby declare that this is my own academic project work, submitted toward the award of

MPhil. Degree and to the best of my knowledge, contains no published material by anyone

to be accepted for the award of any degree of this in any other university, except where due acknowledgement has been made in the write-up or the text.

Student Name & ID. No.

Felix Amfoh .... …........................

(PG4637115) **Signature** **Date**

Certified by:

Dr. David D. Wemegah .... …..........................
(Supervisor) **Signature** **Date**

Certified by:

Prof. Leonard K. Amekudzi ....

…........................

(Head of Department) **Signature** **Date**

ACKNOWLEDGEMENTS

My foremost acknowledgement goes to God Almighty, for the strength, and the undeserved kindness extended to me, throughout the duration of this project work. My sincere appreciation goes to my supervisor, Dr. David Dotse Wemegah for the pieces of advice,

criticism, as well as the motivation and the training, I gained from him. I am indeed indebted to Prof. Aboagye Menyeh, Mr. Thomas Dwomoh (Senior Technician, Geophysics Dept.,) all the staff of the Physics Department. This work would have been impossible, without the great support of Mr. Gilbert Fiadzoe (Senior Technician, Civil Engineering Dept.,) KNUST who took me through the particle size distribution analysis test. Also to the entire staff of the Geotechnical Department of Building and Road Research Institute (BRRI), of the Council for Scientific and Industrial Research, for their collaboration and assistance that enabled the research team to carry out the investigations at the site. I am also greatly indebted to Mrs Ama Tweneboah Tayloy (my dearest supportive sweet Mom), Mr Patrick Tayloy (my sweet Dad), Mrs. Agnes Kankah, (My dearest lovely supportive Mother), Obaapanyin Yaa Effah (My most lovely supportive grand mum), Mr Anthony Appiah, Ms. Gladys Gyasi, Ms. Vivien J. Bediako, Ms. Esther Amfoh and Ms. Portia Naa Teley Sackey for their encouragement, motivation and the enormous advices. Furthermore, I thank Mr. Fiifi Odiansah Turkson of Geomatic Engineering Dept., KNUST, for the software assistance. I also thank Mr. Henry Amoateng, Mr. Francis Boaitey, Mr. Francis Marfo, Mr. Asaph Tei Corletey, and all the MPhil. Students (Physics Department). God richly bless you all.

ABSTRACT

The electrical resistivity tomography (ERT) and the ground penetration radar (GPR) techniques, were employed to characterize the possible lithostratigraphy units at the Kyereyiase clay deposit, in the Atwima Nwabiagya South District of the Ashanti Region of Ghana. The electrical resistivity method was used to measure the distribution of the

resistivity beneath the subsurface thereby providing information about the surface geology. This helped in the mapping of the various lithological units in the study area. The GPR is a non-destructive method that uses electromagnetic radiation in the microwave band of the radio spectrum and detects the reflected signals from subsurface structures at a receiver antenna. This helped in the delineation of the lithological units in the area as well as the depth of the water table. From these results, three main lithological units namely, 5 m thick near surface clay/sandy layer, 20 to 30 m thick weathered granitoids both of which form the saprolite layer and the granitoids bedrock. The water table depth was mapped to ranges from 16 to 20 m. The particle size distribution analysis of soil samples from the area showed that the soil consists averagely of 2 to 24% clay, 8 to 34 % silt, 41 to 86% sand and 1 to 4% gravel. . Similar near surface investigations methods conducted within the study area by the Building and road research Institute (BRRI), under the Council for scientific and industrial research, as well as Ghana geological survey, and other similar research methods of exploring for clay as a subsurface resources, within the Asia and the north America has proving to be very successful for its economical viabilityness.

TABLE OF CONTENTS

LIST OF TABLES

LIST OF FIGURES

CHAPTER ONE

INTRODUCTION

1.1 Background

Primarily, clay is a naturally occurring earth material, with plastic or elastic properties. In Ghana, clay is widely distributed resources occurring in almost all the geological formations. When it comes to industrial and economic importance, it has various applications and usages. Over the years, clay materials have been used in producing household or domestic items, such as pottery and ceramics. In recent times, clay materials have been used in the production line in the housing industry to produce items such as cement, bricks (i.e. ceramic building material), porcelain, paints, paper, chemical filters, floor tiles (Holtz, 1948; Churchman et al., 2006). Clays are well used as a discoloration agent, molecular sieve catalyst and ion exchange, adsorbent, as well as a seal in core of dams due to it impermeable nature. In landfills management, clay serves as a naturally geotextiles or liners, against any toxic seepage (Weems, 1904; Churchman et al., 2006). Therefore, landfills that are constructed in clay rich systems are done without much protective undercover layer (Wemegah et al., 2017). In some cases, the clay is used as covering layer for the prevention of leachate from the landfill when the landfill is decommissioned. These vast uses of clay have led to the increase in the demand for clay. There is therefore the need of adaptation method that can help in the location of the clay deposit to help meet its growing demand in the country.

Primitive exploring and harvesting of clay materials and its minerals have resulted in a negative impact on the environment. Some of these problems include soil erosion, air and

1

water pollution, loss of economic wealth of the soil as well as biodiversity and sometimes geo-environmental disasters. In order to reduce the impact of clay mining on the environment and also get the economic benefit associated with it, there is the need for the adaptation of environmental friendly methods that can help in the location and delineation of the clay deposit site. This will help in the localization of the mining site so as to reduce its impact on the environment.

The use of geophysical methods can help in this regard. The electrical resistivity tomography and the ground penetration radar (GPR) techniques in exploring for earth resources can be employed, as non-destructive means of investigating the subsurface. The resistivity technique, helps in determining the resistivity distribution contrast of various soil types within the subsurface and the depth of various lithological units (Barker, 1989; Banton et al., 1997). This can help in the mapping of the various lithological units. The GPR technique on the other hands, can help in estimating the depth to the bedrock under favourable soil conditions, delineate the stratigraphic architecture, the overburden material, as well as the body geometry (Jol and Bristow, 2003; Sucre et al., 2010). These nondestructive, near subsurface geophysical methods can be useful in the delineation of clay deposit by mapping.

It is in this regard that this collaborative project work, was undertaken between the Department of Physics, KNUST and the BRRI, of the Council for Scientific and Industrial Research (CSIR). This involves the use of these geophysical methods for the lithological study of the Kyereyiase clay deposit in the Atwima Nwabiagya South District of the Ashanti Region of Ghana.

1.2 Problem Statement and Justification

Clays have been used in many civil projects, within the roads and building industries in many countries. In Ghana clay is used in the production of various home utensils, and plays important role in the home. Hence, the availability of clay is important for the growth of these small scale industries that make use of clay. In Ghana, clayey soils are seen in almost all the ten regions. In spite of the long use and benefit of this resources in the country, there are a lot of challenges when, it comes to its mining (Kesse, 1985) thereby leading to the degradation of the environment. These could be due to the fact that there are no proper laid down environmental friendly procedures, when it comes to exploitations of clays in both, small or large scale in the country. Most people adopt primitive ways of mining the clay thereby creating environmental problems or sanity such as deforestation and in some instances depletion of the top soil. Also the inability to know the exact quantity of the clay available in an area, also makes it difficult for proper planning in the use and hence the life span of industries which depends on this raw material for their production.

In order not to lose out of the important role clay plays in the socio-economic development of the country, there is the need for proper and comprehensive approach to the exploration of the clay deposit in the country. The electrical resistivity tomography (ERT) and the ground penetration radar methods, (GPR) were seen to be best suited for this work. These methods have been employed in several related explorations in many countries, for near surface investigations (Wemegah et al., 2017). These methods have the ability to delineate the various lithostratigraphy zones due to their different responses to these methods (Wemegah et al., 2017). These methods are also cost effective, non-destructive and environmentally friendly. The integration of these data sets provided, could help in

3

resolving the many ambiguities that come with geophysical data interpretation. It is in this regard that these methods have been adopted to the mapping of the Kyereyiase BRRI clay deposit, of the CSIR, Furthermore, the success of this project could serve as a basis for similar or related investigations, in the location and quantification of clay deposit in the country.

1.3 Objectives

1.3.1 Main Objective

Main objective of this work is to carry out lithostratigraphy characterization of the clay deposit site.

1.3.2 Specific Objective

The specific objectives of the work are: to use the electrical resistivity and ground penetration methods:

1.   To map the lateral extent and the thickness of the clay deposit.

2.   To determine the depth to the bedrock

3.   To determine the depth to water table.

1.4 Thesis layout

This thesis has five chapters. Chapter one, introduces the main subject, hence stating clearly the background of the research, problem statement and the objectives of the research work. Chapter two talks clearly about the main fundamental theories of both ground penetration radar and the electrical resistivity method and the review of relevant literature. Chapter three gives a review of the geology, of the area, physiography, location and accessibility of

the study area. It also looks at the materials and methods employed in acquiring the data sets. Data processing and enhancement techniques employed were also discussed. Chapter four deals with the analyses and the discussions of the results acquired from the soil sample analyses, electrical resistivity, as well as the ground penetration radar surveys, with detailed interpretations. Chapter five is on the conclusion and gives recommendations for further work in the area.

CHAPTER TWO

LITERATURE REVIEW AND THEORETICAL BACKGROUND

2.1 Application of Geophysical Method

Geophysical resistivity method is typically based on responses of the earth, to the flow of electric current. This method is employed in many subsurface investigations, for mineral resources, ground water exploration, waste mapping, just to mention a few. Reynolds (2011) stated that the electrical resistivity distributions within the ground is based on the physical conditions of the stratigraphy or the lithology. These properties include the mineral composition of the rock, the presence or absence of voids in rocks, porosity, as well as the degree of water saturation. The variation of the resistivity signature based on these properties has made it possible for this method to be applied for exploration for various subsurface materials. Electrical resistivity method has been in use in the area of groundwater exploration as well as subsurface geological characterizations (Barker, 1981; Schmutz et al., 2010; Gazoty et al., 2012; Wemegah et al., 2017). Loke (1999) also has adopted the electrical resistivity technique, for both hydro-geological and geotechnical structures. It is also employed in the fields of mining (Tsiboah and Grant, 2009) and environmental studies (Wemegah et al., 2017). Generally, electrical resistivity technique plays important role in investigating and exploring for the earth resources such as clay materials, coal, as well as mineral resources such as gold (Tsiboah and Grant, 2009). This is based on the fact that these materials produce significant resistivity signatures compared to their hosting rocks. Furthermore, Telford et al. (1990) also reported on a number of research works, where electrical resistivity method was employed in locating and delineating many subsurface resources. It is also used for the study of hydrogeological

features, as well as the mapping of both contaminant and non-contaminant zones (Gazoty et al., 2012; Wemegah et al., 2017). Telford et al. (1976) showed that this method helps in resolving structural features and intruded bedrocks, in unconsolidated sediments.

Other geophysical methods such as the ground penetration radar (GPR) has been used by many geophysicists for subsurface investigation of the earth. The GPR system, operates on the principle of electromagnetic techniques, by transmitting an electromagnetic (EM) wave and receiving the polarized pulses of the EM wave generated beneath the earth subsurface. The generated wave from the GPR technique is dependent on the changes that occur within the electrical properties of the materials within the subsurface. These responses bear the characteristic properties of the subsurface material, such as moisture content, material type or the strata contacts and so on (Reynolds, 2011). This has made it possible for the GPR method to be employed in various field for the subsurface investigation such as exploring for mineral resources, the delineation of zone of groundwater, contaminant zones beneath and waste in the subsurface.

Again, the GPR method has been used by many authors in the lithostratigraphic characterization of the subsurface. Loke (2012), used this method for the investigation of lithostratigraphy identification within the subsurface. Typical example, is that of the subsurface investigation of the stratigraphy recognition,that took place in the Perak, Tronoh and Serilskandar in Malaysia, where layers of some reclaimed sand, were identified within depth of less than 3m. Similarly, lithostratigraphy investigations carried, by Davis et al. (1989), employed the GPR method in the mapping of soil and ground water due to the differences in the dielectric constant produced by the GPR when it comes in contact with

7

these materials. Also, Davis et al. (1989) used GPR method in delineating sandy soil layers and clay layers beneath the earth surface. Furthermore, the GPR technique has been, employed in probing into the electrical properties of most geologic materials or bodies that occur naturally.

With the GPR method, the electrical conductivity and the dielectric polarization of these naturally occurring materials can be known. Huggenberger et al. (1993) have done researches in which the GPR method was applied in investigating the geologic structures such as fractures, faulting, folding and jointing in the subsurface. Also, GPR method has been utilized in resource mapping in coal mines (Davis et al., 1989).

2.2 Electrical Resistivity

2.2.1 Basic Theory of Electrical Resistivity

Electrical resistivity measurement, beneath the surface of the earth is primarily based on the principle that, the distribution of electrical potential beneath the earth, around a currentcarrying conductor is depended on the electrical resistivity distribution of rocks and soils. Hence, electrical resistivity measurement provides information about the resistivity distribution within a geologic formation. The main theory governing the electrical resistivity measurements is the Ohm's law (Kearey et al., 2002), which is dependent on how the electric potential responds to injected current flow through a conducting medium. The potential difference aids in providing vital information, concerning the subsurface heterogeneities as well as its electrical properties or characteristics (Kearey et al., 2002).

8

Figure: 2.1 is an illustration of an element of homogeneous material carrying a current through a cylinder, causing a potential drop -▢v at both sides of the element. Mathematical illustration of Ohm's law indicating a current flow through a conductor, is proportional to the voltage across the conductor,

$$\delta v \; \alpha \; I \; - - - -(1)$$

This can be, rewritten as:

$$\delta v = R\delta I \; ---------(2)$$

R (i.e. the constant of proportionality), which is the resistance of the conductor that opposes the flow of current in the material medium.
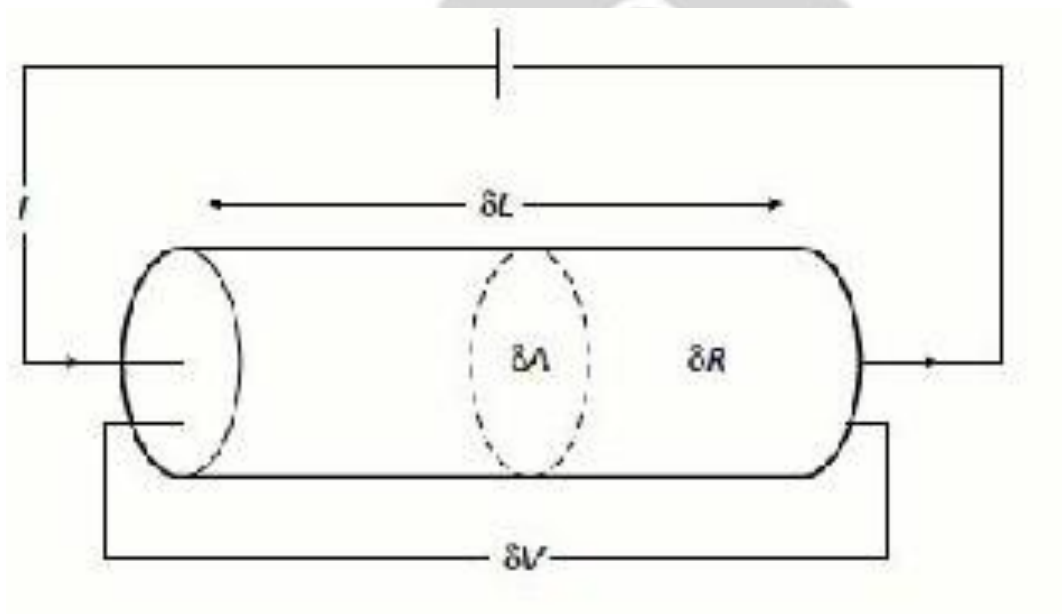
Figure: 2.1 indicating Resistivity of an element cylindrical material (Modified after: Kearey et al; 2002).

From the figure 2.1, it can also be shown that the resistance δR is proportional to the length ▢L, and inversely proportional to the cross-sectional area, ▢$A$of the conductor,

9

$$\square R\alpha\frac{\delta L}{\delta A} - - - - - - (3)$$

$$\square R = \rho\frac{\delta L}{\delta A} - - - - - (4)$$

Where ρ is a constant of proportionality refers to as the resistivity of the material. In definition, the resistivity (ρ) is the resistance of 1 Ohm between the opposite faces of a cubic material (Kearey et al., 2002). It is a physical property of a material that expresses its ability to oppose current flow through it. The standard unit for resistivity is the Ohmmeter (Ωm). The reciprocal of the resistivity which is the conductivity$\square\square\square$, is given as:

$$\sigma = \frac{1}{\rho}$$

By substituting for δR in equation (4 with that and re-arranging, the equation becomes

$$\frac{\delta V}{\delta L} = -\frac{\rho I}{\delta A} = -\rho J \text{--- --- --- --- } (5)$$

With $\dfrac{\square v}{\square L}$ being the potential gradient through the element in Vm^{-1}. In general, the current density within a media, in any direction, is the negative partial derivative of the potential in that direction, divided by the resistivity. In relation to current density (J), the electric field intensity (E) and the conductivity$\square\square\square$, the ohm's law can be written as:

$$J = \sigma E \text{-------------------}(6)$$

2.2.2 Equipotential Distribution of Current in the Ground.

Considering a homogeneous and an isotropic half – space, the electric field lines that encompasses a source electrode, which serve as a power source to the subsurface earth is radially directed outwards, producing surface hemispherical (Scollar et al., 1990; Kearey et al., 2002) as shown in figure 2.2. The potential distribution around appositive source,

1 often reduces by ⌐, as the distance increases. As it goes round the negative electrode r

(sink), the potential increases as $\dfrac{1}{r}$, with increasing distance from the sink.
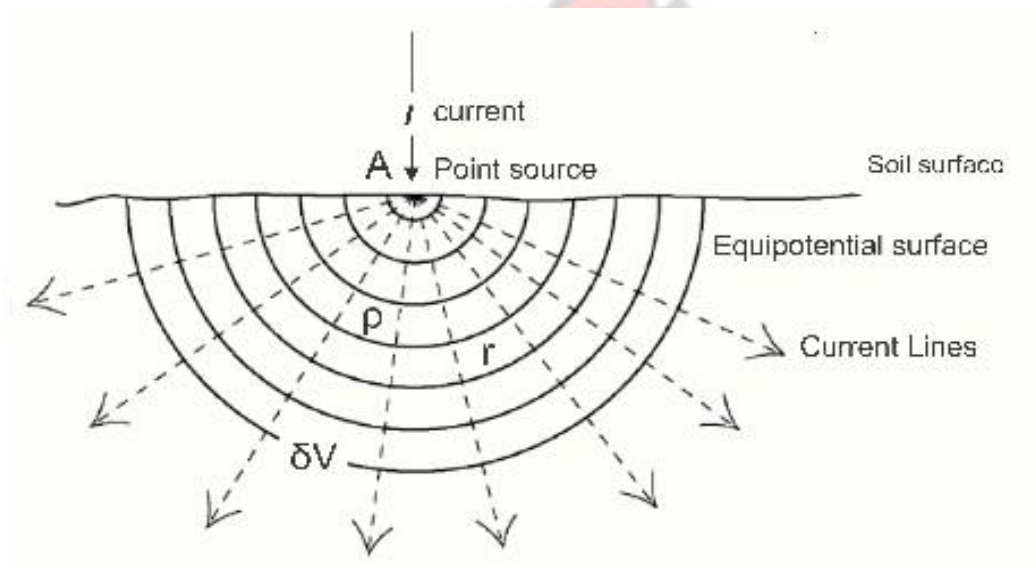
Figure 2.2: Current flow distribution in a homogeneous soil from a single electrode. (iModified after Scollar et al., 1990; Kearey et al., 2002)

In general, the current density within a media, in any direction, is the negative partial derivative of the potential in a direction, divided by the resistivity, hence the physical parameter measured in the field is the electric potential (V) as related to the electric field as

$\square \ \square\square\square \ \square E \ V$ (7)

Therefore, by combining equation (6) and (7).

$$J \ \square \ \square\square \ v \ \text{----------------(8)}$$

11

With the distance (r) from the electrode, the shell surface area as $2\pi r^2$, hence the current

density (J) is given as:

$$J = \frac{I}{2\pi r^2} ----(9)$$

Therefore

$$\frac{\delta v}{\delta r} = -\rho J = -\frac{\rho I}{2\pi r^2} - (10)$$

Hence, integrating equation 10, using integration constant of V = 0 when r $\Rightarrow \square$, gives

$$v = \frac{\rho I}{2\pi r} - (11)$$

2.2.3 Electrode array and Geometrical coefficient

The field based electrical resistivity survey is often carried out, with four or more

electrodes. As shown in Figure 2.3, where A and B are current and C and D are the potential

electrodes.
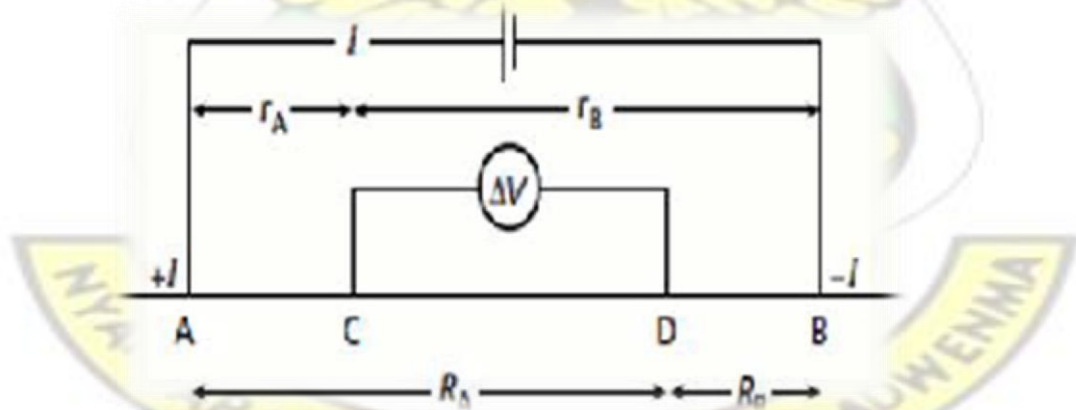
Figure: 2.3 Electrode configuration employed in an electrical resistivity measurement, with
A and B being the current electrodes and C and D being potential electrodes.
(Modified after: Scollar et al., 1990; Kearey et al., 2002)

Considering that the sink is at a finite distance, from a source (Figure 2.3), the potential Vc at electrode position C, is the sum of the potential contributions V_A and V_B from current sources A and the sink B. Hence

$$V_C = V_A + V_B$$

$$V_C = \frac{\rho I}{2\pi}\left(\frac{1}{r_A} - \frac{1}{r_B}\right)$$

Similarly, at D

$$V_D = \frac{\rho I}{2\pi}\left(\frac{1}{R_A} - \frac{1}{R_B}\right)$$

The potential difference (between the electrodes C and D is obtained as

$$\nabla V = V_c - V_D = \frac{\rho I}{2\pi}\left(\left(\frac{1}{r_A} - \frac{1}{r_B}\right) - \left(\frac{1}{R_A} - \frac{1}{R_B}\right)\right)$$

The equation can further be rearranged in the form

$$\rho = \frac{2\pi\nabla v}{\left[\left(\frac{1}{r_A} - \frac{1}{r_B}\right) - \left(\frac{1}{R_A} - \frac{1}{R_B}\right)\right] I}$$

If

$$k = \frac{2\pi}{\left[\left(\frac{1}{r_A} - \frac{1}{r_B}\right) - \left(\frac{1}{R_A} - \frac{1}{R_B}\right)\right]}$$

Where k is the geometrical coefficient, with ρ_a being the apparent resistivity, then

$$\rho a = \frac{k\nabla v}{I}$$

13

2.2.4 Basic Electrode Arrays

Many configurations have been designed for electrical resistivity measurement on the basis of the arrangement of the potential and current electrode separations (Habberjam, 1979). These configurations include: The gradient, Wenner, dipole-dipole, dipole – pole, pole – pole, as well as the Schlumberger arrays. The equations use in the calculation of apparent resistivity for these electrode arrangement are as follows with

a = Electrode separation   n = Any arbitral number given, such as 1…5

1   **Schlumberger Array**

a. $\rho_a = \pi n(n+1)a \left[\dfrac{\Delta V}{I}\right]$

2   **Wenner   Array**

$\rho_a = 2\pi a \left[\dfrac{\Delta V}{I}\right]$
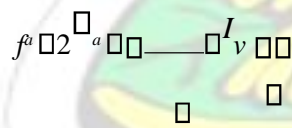
3   **Dipole –dipole Array**

i. $\rho_a = \pi n(n+1)(n+2)a \left[\dfrac{\Delta V}{I}\right]$

4   **Pole - Dipole**

$\rho_a = 2\pi na(n+1) \left[\dfrac{\Delta V}{I}\right]$

5   Pole – pole Array

$$f_a \square \square na \square \square \underline{}$$

$$\square Iv$$

$$\square \square \square \ \square$$

$$f_a \square \square_{na} \square n \ \square 1 \square \underline{} \square v$$
$$I$$

The adaptation of any of these electrode configurations for exploration purposes depend on many factors. Among the key factors, involved in selecting a protocol or array include, the rate of survey, background noise and the sensitivity of resistivity among others (Loke, 2001).

2.2.5 Modes of Electrical resistivity surveying

In generally, two main techniques are employed during electrical resistivity data acquisition on the field. These are the vertical electrical sounding (VES) and profiling. The vertical electrical sounding is used for depth sounding. It is used in exploring, for the vertical variation in resistivity, within the subsurface earth. Profiling on the other hand is employed in determining the horizontal variation of resistivity along a profile. In addition to these two modes, an approach called the continuous vertical electrical sounding (CVES), which employs the characteristics of VES and CST in its operation is also used. Figure 2.4shows the application of this mode on a field scale survey.
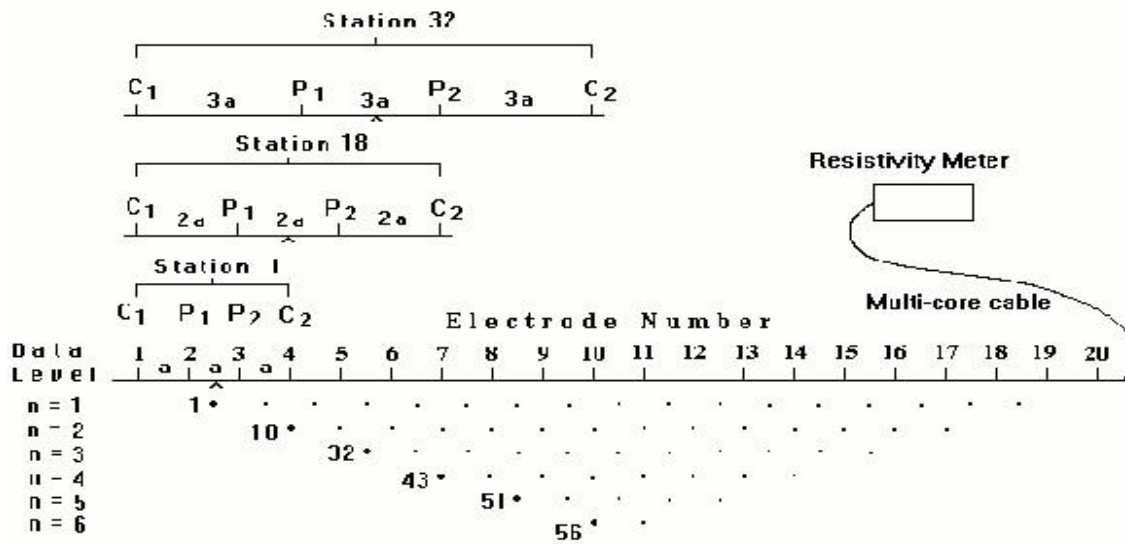
Figure: 2.4 illustrating the sequence of measurement to build up a pseudo-section.
(Modified after: Reynolds, 2011).

2.2.6 Electrical Resistivity of Rock and Minerals

The variation in the electrical properties of an earth materials helps to produce changes between the applied current and the potential readings. Rocks and soils is generally not good conductors, and are or it mainly carry current through the fluids pores. The electrical current mainly gets transmitted, due to the passage of ions in the pore water, as a form of electrolytic processes. Generally, sedimentary rocks are the most conductive, due to their high fluid content, metamorphic rocks are the intermediate, with overlapping resistivity, whiles igneous rocks have the highest resistivity. Therefore, electrical resistivity of soils, are the function of the soil properties, which may include the mineralogy and particle size distribution, conductivity, degree of water saturation and pore size distribution and porosity. Figure 2.5 Show the range of resistivity and conductivity of different earth materials.
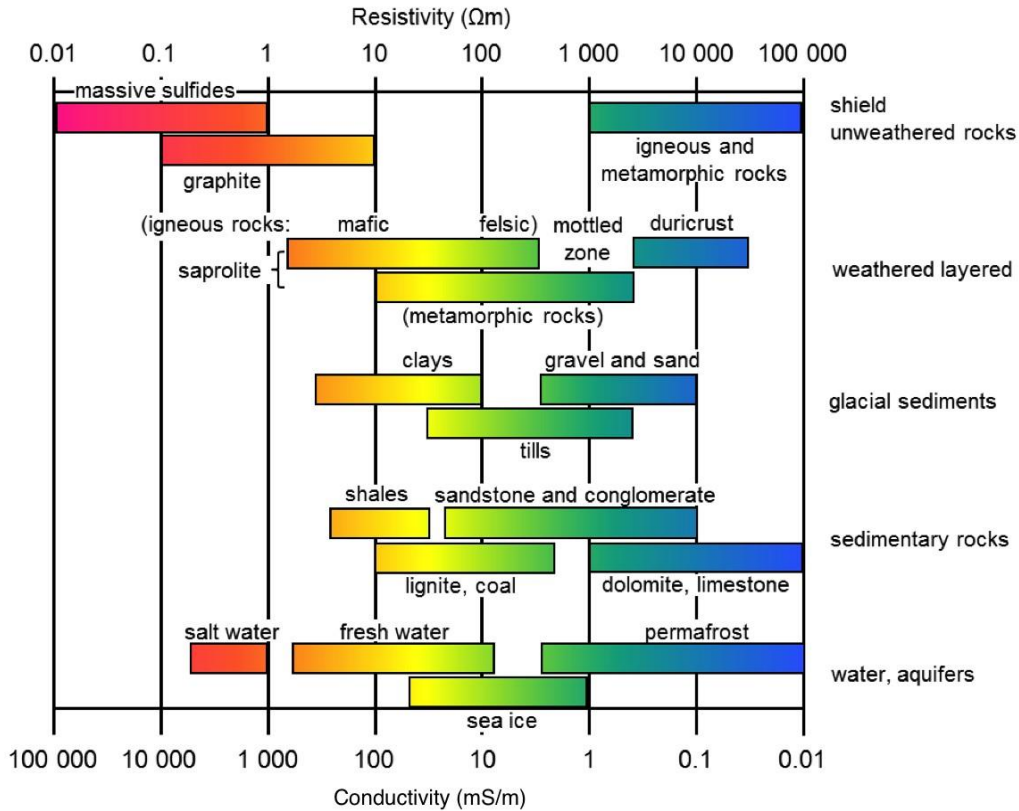
Figure: 2.5 Resistivity of various rocks and minerals (Modified after: Reynolds, 2011).

2.3 Basic GPR Radar Theory

Radio detection and ranging (RADAR), employs the transmission of short signals of radio frequency electromagnetic energy beneath the earth's subsurface. This non-destructive method uses electromagnetic radiation in the microwave band of the radio spectrum, and detects the reflected signals from the subsurface structures. This method operates, mostly on the propagation and the reflections of the electromagnetic energies generated within the subsurface of the earth's crust. The energy produced by the transducer, travel through the earth's subsurface in a form of a broad band electromagnetic wave which is intercepted by materials of varying dielectric properties producing a reflected wave. The reflected EM

wave is received on the surface by the help of the receiver antenna. This is processed and displayed as a radargram. This helps to give information relating to the subsurface.
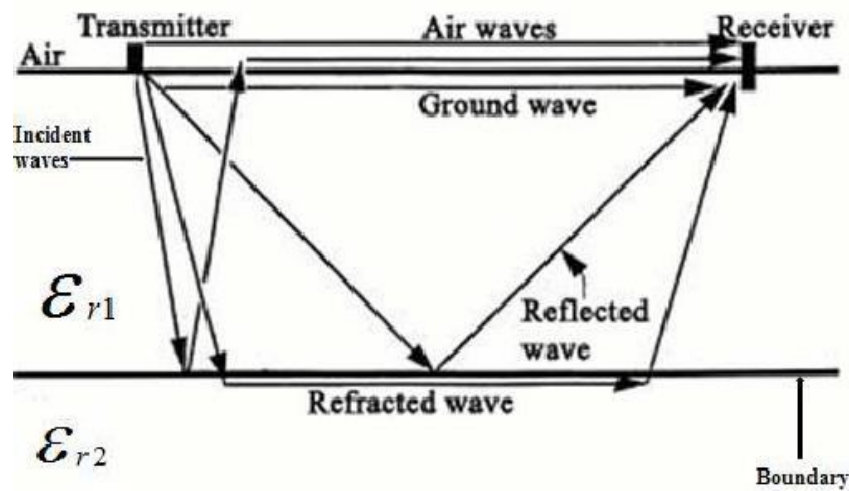
Figure: 2.6 Electromagnetic Wave Propagation through a medium (Modified after: Scollar et al., 1990; Kearey et al., 2002)

The electromagnetic wave behaviour, within a medium of propagation is dependent on the properties, such as magnetic permeability dielectric permittivity (Ɛ) and electric conductivity (Huggenberger, 1993; Brewster and Annan, 1994; Fokkemaet al., 2001; Preko, 2007; Preko and Wilhelm, 2012). These make it possible for this method to be employed in geological environment for mapping of lithological variation in the subsurface.

The propagation velocity (v) of the electromagnetic wave can be represented by

$$v \; \square \; \frac{1}{\sqrt{\square\square}}$$

18

For electromagnetic waves, the velocity v can be given as

$$v = \frac{1}{\sqrt{\varepsilon_o \varepsilon_r \mu_o \mu_r}}$$

Where $\varepsilon_o, \varepsilon_r$, μ_o, μ_r , denote electric permittivity of free space, relative dielectric permittivity, magnetic permeability of free space and relative magnetic permeability respectively.

This equation can be written as

$$v = \frac{1}{\sqrt{\varepsilon_o \mu_o}} \cdot \frac{1}{\sqrt{\varepsilon_r \mu_r}}$$

Where $c_o = \frac{1}{\sqrt{\varepsilon_o \mu_o}}$ is the speed of the electromagnetic wave in vacuum or free space.

Hence,

$$v = c_o \cdot \frac{1}{\sqrt{\varepsilon_r \mu_r}}$$

$$v = \frac{C_o}{\sqrt{\varepsilon_r \mu_r}}$$

But for most earth materials, μ_r equal to one, therefore the equation becomes:

$$v = \frac{c_o}{\sqrt{\varepsilon}}$$

19

$$\square_r$$

Given that, $C_o= 3.0 \times 10^8\, m/s = 0.3\, m/ns,$ then v can be written as

$$v \square \frac{0.3}{\sqrt{\square_r}}$$

This equation shows that relative dielectric permittivity is the single most important parameter needed to determine the velocity of propagation of an EM wave through any geological medium. Table 2.1 shows the list of some rocks and their relative permittivity and attenuation values.

Table: 2.1 Materials attenuation and relative permittivity (Reynolds, 1997; Daniels, 1996)

Materials	Attenuation (dBm^{-1})	Relative permittivity ($\square_r$)
Clay	10 – 100	2-40
Granite: dry	0.5 – 3	5
Granite: wet	2 - 5	7
Lime stone: dry	0.5 – 10	7
Limestone: wet	10 –2 5	8
Sand: saturated	0.03-0.3	10-30
Sand stone: dry	2-10	2-3
Sand stone wet	10-20	5-10
Soil: firm	0.1-2	8-12
Soil: sandy dry	0.1-2	4-6
Soil: sandy wet	1-5	15-30
Soil: loamy wet	1-6	10-20
Sandy: dry	0.1-2	4-6
Soil: loamy dry	0.5-3	4-6
Soil: clayed dry	0.3-3	4-6

Soil: clay wet	5-30	10-15

2.4 CLAY

The term clay refers to a naturally occurring material composed primarily of fine-grained phyllosilicate minerals which is generally plastic with appropriate water contacts and harden, when dried or fired. Clay is soil that has grain size less than 0.002 mm as in (Figure 2.8) (Daniels et al., 2008).

. There are two main classification of clay, namely

1.   Residual or Primary Clay: these are clays formed at the site of the parent rocks.

2.   Secondary Clay: These are clays that are transported from multiple sources by water (Alluvial) or wind (Aeolian). The secondary clay minerals, often known as the phyllosilicates, are the most important components of most crystalline layered structure. Generally, isomorphism and polymorphism are common in the phyllosilicates, as a result of the octahedral sheet.
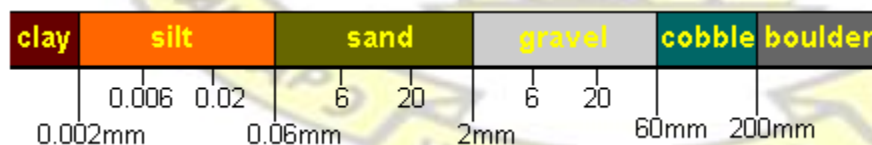
Figure: 2.7 Indicating Soil Classification (Separation) and size limits (sieve size) (Modified after: Daniels et al., 2008)

2.4.1 Formation and alteration of clay material.

Clays and clay minerals occur under a fairly limited range of geologic conditions. The environments of formation include soil horizons, continental and marine sediments, geothermal fields, volcanic deposits, and weathering rock formations. Most clay minerals form where rocks are in contact with air, water, or steam. Therefore, the nature of clay formed during the weathering process depends on factors such as the mineralogical and textural composition of the parent rock, the composition of the aqueous solution, and the nature of the fluid flow. The contact of rocks and water, produce clays, either at or near the surface of the earth (Daniels et al., 2008). For example, the (CO_2) gas can dissolve in water to produce hydrogen ions (H+) and bicarbonate ions, and make water slightly acidic as shown in the equation ($CO_2 + H_2O => H^+ + HCO_3^-$) The acidic water reacts with rock surfaces and tends to dissolve the (K) ion and silica from the feldspar. Finally, the feldspar is transformed into kaolinite. Hence, the rock mineral weathering becomes one of the main natural sources of clay formation within the entire soil mass.

The formation and alteration of clay minerals and their accumulation as clay materials can occur by a very wide range of processes. Most of these processes and the environments in which they operate involve the chemical actions and physical movement of water. As such, clay minerals can be considered as characteristic minerals of the earth near surface hydrous environments. This includes weathering, sedimentation, low-grade

metamorphism and hydrothermal alteration, as shown in   Figure 2.8. Clay and its mineral such as smectite, montmorillonite and illite occurs as a result of gradual chemical weathering of rocks, which are typically silicate-bearing, with low concentrations of

22

carbonic acid. Collectively, the formations of clay and it associated minerals comes as a result of two major phenomena called the supergene and the hypogene processes. Generally, clays formed from the supergene processes occurs near surface earth that really requires a long period of time for formations, with some acceleration conditions. However, under some   situations, supergene activities such as deposition and leaching, coupling with weathering, brings about clay soil formation. But with the hypogene clay formation, the processes come as a result of actions that occur at the subsurface gases, vapors and solutions that forces its way upward through fractures or cavities found within the earth's crust. In line with these processes, the main materials that comes as a result of the processes are alumina, silica, alkali earth elements and iron. (Merriman, 2006).

Figure 2.8 is a typical clay forming cycle.
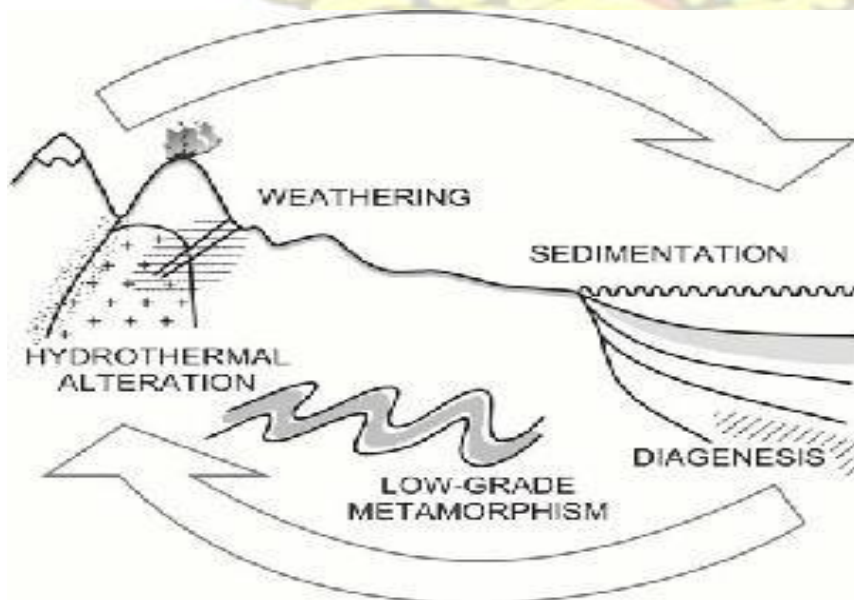
Figure: 2.8 Schematic clay cycles, whereby clay minerals formed in one environment are frequently recycled into others (Modified after: Merriman, 2006)

In this cycle, clay and its minerals are formed at a temperature range of 100-450°C in an acidic, alkaline and neutral environment, depending on the source material such as the P^H of the magma that contains the invading vapours. (Kesse, 1985). Generally, clay deposits found in Ghana belong to the supergene or the weathering product type with their property depending on the parent rock. (Merriman, 2006). The clays that weathered from schist and phyllite are usually very plastic with kaolinite and illite being the main clay minerals. But those formed from granite are non-plastic, and contains predominantly quartz with little kaolinite. Whiles those from shale are very plastic with montmorrilonite and illite as the major clay minerals (Figure 2.9). Kesse (1985) also stated that, the chemical decomposition of feldspar, contributes to the process of clay formation.
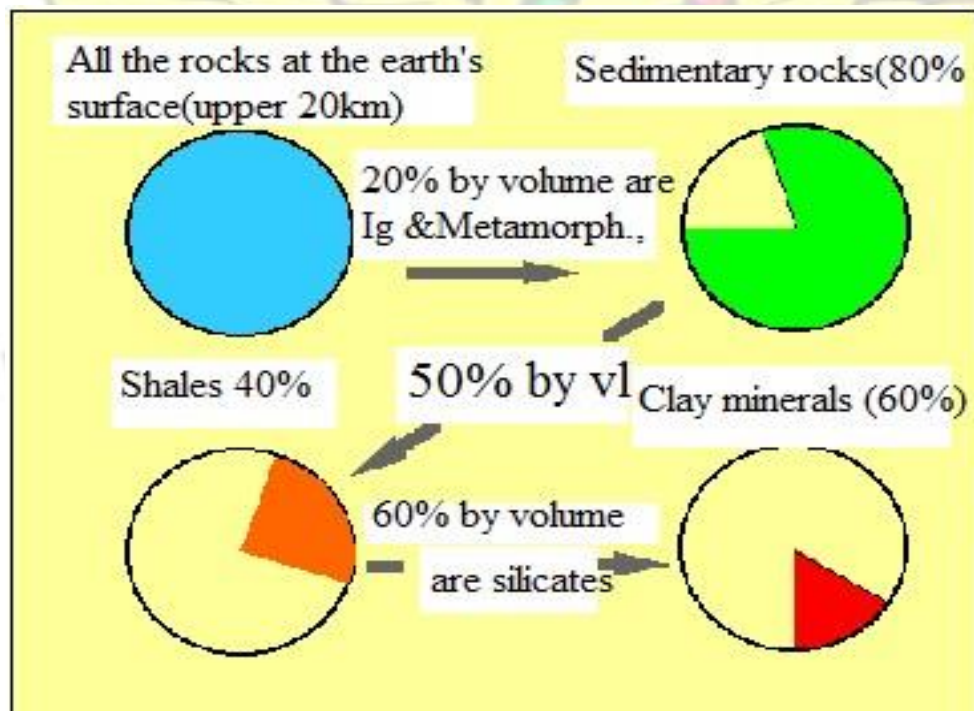
Figure 2.9: Illustrating percentages of some clay rocks and its minerals (Modifies after: Merriman, 2006).

2.4.2 GRADATION OF SOIL SAMPLING

In order to determine the composition of clay in any soil sample, there is the need for particle size distribution analysis of the sample. This is mostly performed to determine the percentage different grain sizes within soils. Gradation or particle size distributions analysis can be described as the proportions by dry mass of a soil distributed over specified particles size ranges. Particle size distribution is influenced by the current depositional of the medium (water or other fluids) that deposited the soils. Knowing the grain size distribution of a soil is important for a variety of reasons. For instance, with the help of particle size distribution, civil and geotechnical engineers are able to design and make recommendations regarding projects such as, water drainages, dams, bridges and building foundations. Similarly, geologists are able to determine the depositional provenance within the environment. Also, particle size distribution (PSD) in soil is among the most fundamental source of physical properties of soil, as it is most widely employed for drawing estimation of soil hydraulic properties, such as the water-retention curve, saturated, and unsaturated conductivities (Kesse, 1985)**.**

With conventional particle- size analysis, the mass fractions of sand, clay and silt can be achieved. Hence these can be of help, in finding the textural class, through the textural diagram, in a form of textural triangle Kesse (1985).

2.4.2.1 Grain Size Analysis

The sieve analysis is often used to determine the grain size distribution of coarser or largesized particles, while the hydrometer method is used in the determination of the distribution of finer particles standard reference. This analysis is performed using the

25

American Society of Testing and Material (ASTM –D 422 for particle -size analysis and standard test method for soils) standard. Per the international standard of testing subsurface materials, the larger size or the coarser grain size, greater than 2 mm, but less than 63 mm were considered as gravels, whiles grain size less than 2 mm but greater than 0.06 mm were considered to be sand. Also, grain size less than 0.06 mm but greater than 0.002 mm, were considered as silt, with those particles size, less than 0.002 were considered as clay.

2.4.3 Industrial uses of Clay

The use of clay depends on its property. Fire clays are used for manufacturing refractory products such as heat-resistant tiles or bricks. The ball clays are used for Ceramics, filers and drug manufacturing, as well as for paper coating and fiberglass. China clay (predominantly, Kaolinite) is used for ceramics, filer and drug manufacturing, as well as for paper coating and fiberglass, with Smectite (bentonite) used as drilling muds. Expanded clays are used for manufacturing of expanded clay blocks for insulation, as well as cements. Major clays are used for brick and cement manufacturing. Clay, has also been used as pozzolanic material. It has also been proven that pozzolanic clay when mixed with cement helps improve the stability of the cement since it reacts with hydrated products. Furthermore, clay has over the years been used by man, for most of our existence and for other miscellaneous objects such as water filtration systems, paper making, various ceramics products, building bricks, cement, and many more, throughout history. In line with these, the BRRI, have over the years been employing the various clays in coming out with both raw pozzolana and mixed pozzolana cement products. This product is widely used in the construction industry in Ghana for making concrete mortal for civil works.

26

CHAPTER THREE

MATERIALS AND METHODS

3.1 Summary Description of the geophysical methods used

The electric resistivity methods play important role in the mapping of subsurface structure sand the geologic stratigraphy. In the electrical resistivity methods, current is injected into the ground through steel electrodes, after which the bulk resistivity of the subsurface is recorded with the aid of an ABEM LUND Terrameter The ground penetration radar methods, employed transmitter that emits pulses of high frequency electromagnetic waves into the earth's subsurface. The electromagnetic wave is then reflected when it encounters media of changing dielectric permittivity of the subsurface. The electromagnetic energy is reflected back to the surface by a receiving antenna, which is later recorded as a function of time. The depth of penetration of the ground penetration (GPR) is severely limited by the attenuation and the absorption of the transmitted electromagnetic waves into the ground. Hence the penetration of the radar waves is reduced by a shallow water table, high clay content of the subsurface in the areas where the electrical resistivity of the subsurface is less than thirty (30) ohmmeters. (Reynolds, 2011). These two geophysical methods were adopted to the lithostratigraphic characterization of the Kyereyiase clay deposit site in the Atwima Nwabiagya South District, Ashanti Region.

3.2 Study Area

3.2.1 Project Site Description

The study area is located at Kyereyiase in the Atwima Nwabiagya South District of the

Ashanti Region. The Atwima Nwabiagya District lies within latitudes $6^o75^{'}$ N and 6.67 N and longitudes $1^o45'$ W and 1.81^oW. It covers an estimated land mark area, of 294.84 km square with estimated average population of 14,902 as at the year 2010 (Ghana Statistical Service, 2012,2010). The Kyereyiase Community is about 8 km from the district capital and 15km from the regional capital, Kumasi. It covers less than 1% of the landmass of the Atwima Nwabiagya Districts (Atwima Nwabiagya District Assembly Report, 2013) The site is located at the bank of the Offin River. The project site is partly masher area, with sandy soil and clayey materials as the dominant soil deposit.

Figure: 3.1 Location and accessibility of the study area. (Generated map of Atwima Nwabiagya District Assembly) (Source: ArcGIS, 2013, Version 10.6)

3.2.2 Climate and Physiography

The area has two main raining seasons, the major season from March to July and the minor season from August to mid-November. The average rainfall, ranges from 170cm to 185cm per year and average temperature ranges between 27ºC to 31ºC.The average relative humidity in the area is approximately ninety-three percent. The average topographical elevation is about187 m above mean sea level, with the high lands, having gentle to steep slopes. The Tano Owabi and the Offin rivers, are the main rivers within the district.

3.2.3 Vegetation

The vegetation seen within the Atwima Nwabiagya Districts is the pre-dominantly semi – deciduous forest. The forests have been disturbed by all kinds of bad human activities, such as, sand winning, improper clay mining, by both individuals and BRRI as an institution and the constant logging for charcoal productions. These activities have led to the destruction of the districts important biodiversity.

3.2.4 Geological Setting

3.2.4.1 Regional Geology

Kyereyiase is located within the Ashanti-belt, and forms a significant portion of the stratigraphy of the Ashanti-belt, in south-western Ghana. The Ashanti-belt is a northeasterly striking, broadly synclinal structure and geologically, made up of lower Proterozoic metavolcanics and metasediments of the Birimian Supergroup. The formation is overlain unconformably by the Tarkwaian1Formation, which is characterized by lower

29

intensely metamorphism rocks. Also associated with formation, are granitoids complex refer to as the Birimian granitoids complex.

3.2.4.2 Proterozoic Birimian Supergroup

In Ghana, the Birimian Supergroup have been divided into two units namely the metasediment which has sedimentary origin and the metavolcanic unit comprises metamorphosed basic, and intermediate lavas, as well as pyroclastic rock formations (Junner, 1935). The metavolcanic units are mostly basalts with interflow sediment (Eisenlohr and Hirdes, 1992). The metasedimentary units consist of an assemblage of finegrain size rocks, with large volcanoclastic constituents. Lithologically, the metasedimentary unit consists of as greywacke, siltstones, phyllites, tuff, shale, as well as some chemical (Mn-rich) sediments.

3.2.4.3 Birimian Metavolcanics

The Birimian basically comprises volcanic belts and among these include the Amphibolites or the greenstones, Ashanti Calcareous chlorite-schists, and the Kibi-Winneba belt. Minor intrusions of mafic rocks cut the volcanics, with some interbedded sediment occurring within the basaltic flows of the volcanic belts (Leube et al., 1990; Leube et al, 1986). Metamorphism processes that occur in most this volcanic rocks are often confined to the chlorite zone of the greens schist facies, with Amphibolite-facies assemblages occurring sporadically but especially along the margins of granitoid rock formations.

3.2.4.4 Birimian Metasediments

In Ghana, the Birimian Metasedimentary rocks are classified into: (I) chemical sediments

(II) argillitic rocks (III) turbidite-related greywackes and (IV) volcanic clastic rocks. Generally, the boundaries that comes along with these subdivisions are gradational. The volcano-clastic sediments mainly consist of sand-silt-sized, with partly re-worked pyroclastics, that is shown by the presence of chloritised glass fragments, idiomorphic plagioclase crystals, quart and with the absence of heavy minerals (Leube et al., 1990).

3.2.4.5 Birimian Granitoids

The Eburnean granitoids found in the Birimian differs in terms of age, mineralogy and chemistry. This includes the late K-rich (G3 type granitoids) consisting of the Banso, Bongo and the Tongo granitoids, the belt type granitoids found mainly within the volcanic belts are often dominated by hornblende bearing granites. The sedimentary basins type granitoids (G1), which are found within the sedimentary basin with the Kumasi Batholith been one of such deposit (Kesse,1985). Further, research works have also proven that granitoids rocks are noted to be in areas that have undergone crustal thickening during orogenics. (Kesse,1985; Leube et al., 1990).

3.2.4.6 Local Geology

The Atwima Nwabiagya District is underlain by the Birimian rock formation, which is characterized by lithologies such as the basin granite, schist, greywacke and phyllites. Economically, these rocks are considered very important due to their good clay deposit for bricks and ceramics. The basin granitoid is used mainly in the building and road construction industry.

3.2.4.7 Soils of the study area

The Bekwai-Nzema loda complex association and the Nsuta-Offin/Kumasi-Asuani Compound association are among, the predominant soils confined in the District. Comparatively, the soils consist of a fairly high moisture holding capacity, with some marginal mechanical properties such as high plasticity. The Kumasi-Asuansi Compound association is believed to have come from areas, such as Toase, Abuakwa, Nkawie and

Nehebehi (Atwima Nwabiagya District Assembly, 2013).

3.3 Method

3.3.1 Resistivity Survey

The electrical resistivity method was employed for the investigation into the subsurface for possible lithostratigraphy characterization of the study area. The electrical resistivity method had been used in the exploration for both shallow and deeper sections of the subsurface. Since its origin in the 1920's, by the Schlumberger brothers, the electrical method has been employed for interpretation, quantitative, and conventional sounding survey (Barker, 1981).

3.3.1.1 Materials

Materials and Equipment used for the electrical resistivity data acquisition includes:

1.   The ABEM Terrameter with the LUND Imaging system,

2.   Global positioning system (GPS)

3.   Electrodes, jumpers, hammers, cables and

4.   12v Li-ion car battery

5.   Res2dinv software

6.   Source: ArcGIS, 2013

Figure 3.2: Pictorial view of the ABEM LUND Imaging system and its various components (Modified after: Reynolds, 2011)

3.3.1.2 Resistivity Data Acquisition using ABEM Terrameter

The Geophysical instrument employed for the resistivity data collection is the ABEM LUND Imaging system. The main component of the setup is the Terrameter SAS400 that operates on an automated electric imaging component. Although, there have been other inventions, the ABEM LUND imaging system is still regarded as one of the state of the art, resistivity/IP surveying device for the geophysical investigations of the subsurface. The ABEM Terrameter with the Lund imaging device system was operated with the multielectrode system. For the data acquisition, at the project site, sixty-one (61) electrodes were aligned in a straight profiling, with the help of a Brunton Compass, using electrode spacing of 2 m. After the electrodes were planted in the ground, and the jumpers, fixed to

its respective take-out position to the multi-core cable, the electrode selector unit was automatically selected for the data acquisition. The system was powered using a 12 v battery.

The electrodes used as current or potential pairs are determined by the selector. The Terrameter then measures the apparent resistivity values from the different electrodes and the value plotted at the midpoints of the two electrodes used. The process was repeated until all the data corresponding to the various midpoints of the electrodes were measured. For profiles that were longer than 160 m, the setup was rolled along to cover the whole profile length.

3.3.1.3 Resistivity Data Processing and Inversion

The processing of the resistivity data obtained from CVES involves the use of a RES2DINV software which provides a qualitative interpretation to the data. In processing the field data, the data was filtered to enable any bad data point in a form of spike to be removed. The bad data points have either too low or high resistivity values as compared with its surrounding datasets. Extermination of these data points were done to remove data that are considered to be of poor quality. The spikes on the pseudo-section can occur due to poor contact between the electrode and the ground or electrode failure due to shorting of cables (Loke et al., 2001). By gradually removing the bad data point one by one, the quality of the data is enhanced. Removal was done by clicking on the spikes which led to the selection of the bad data points which then appeared as spikes with 'red' dots (Figure 3.3) and then deleted. The data were then inverted which transformed the apparent resistivity

into model or pseudo-section that displayed the subsurface resistivity distribution of the earth (Loke, 1999; Loke and Barker, 1996).
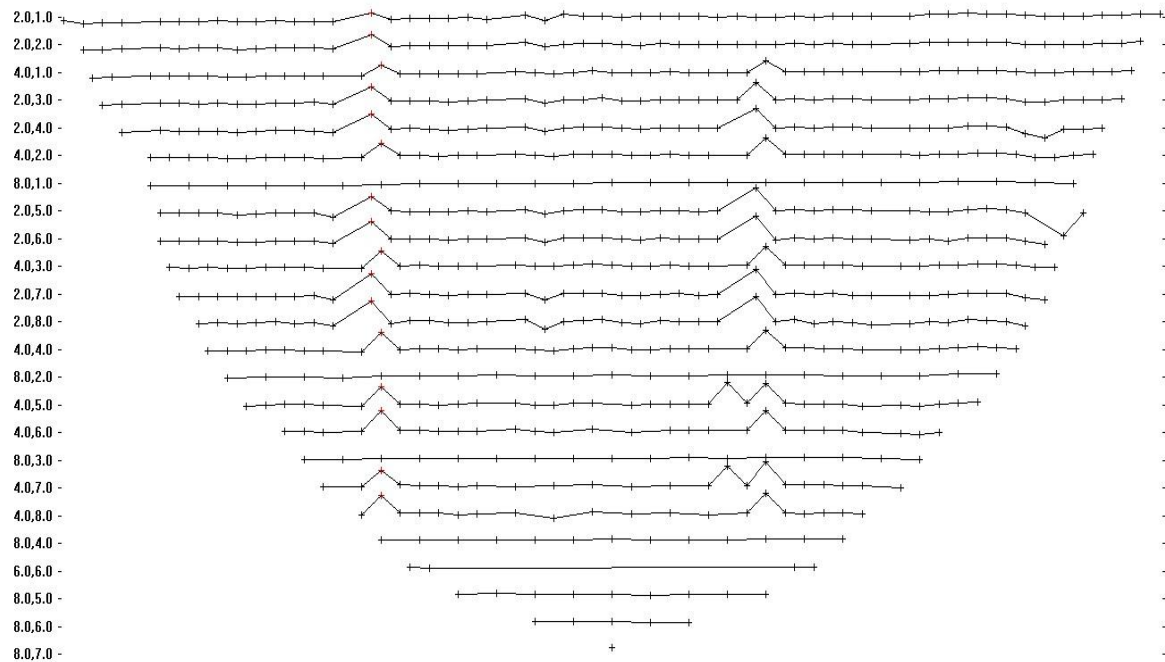
Figure 3.3: Pseudo-section showing bad data points indicated with Spikes(Source:Res2dinv software)

3.3.2 GPR Survey

3.3.2.1 Materials and Equipment Used for the GPR survey

In the ground penetration radar data collection, the Mala GPR System (Fig.3.4) was employed. The device consists of XV monitor, antenna unit (Mala Unshielded Rough Terrain Antenna) and the Mala ProEx control unit. The mala rough terrain antenna (RTA) which operates, on the basis of the ProEx system, is specifically made for low frequency surveying or investigations. The mala XV Monitor serves as a platform for the data acquisition (Fig.3.4). A standard 12V Li-Ion batteries were used in powering the GPR devices. The main software used in the processing of the data is the ReflexW.

35
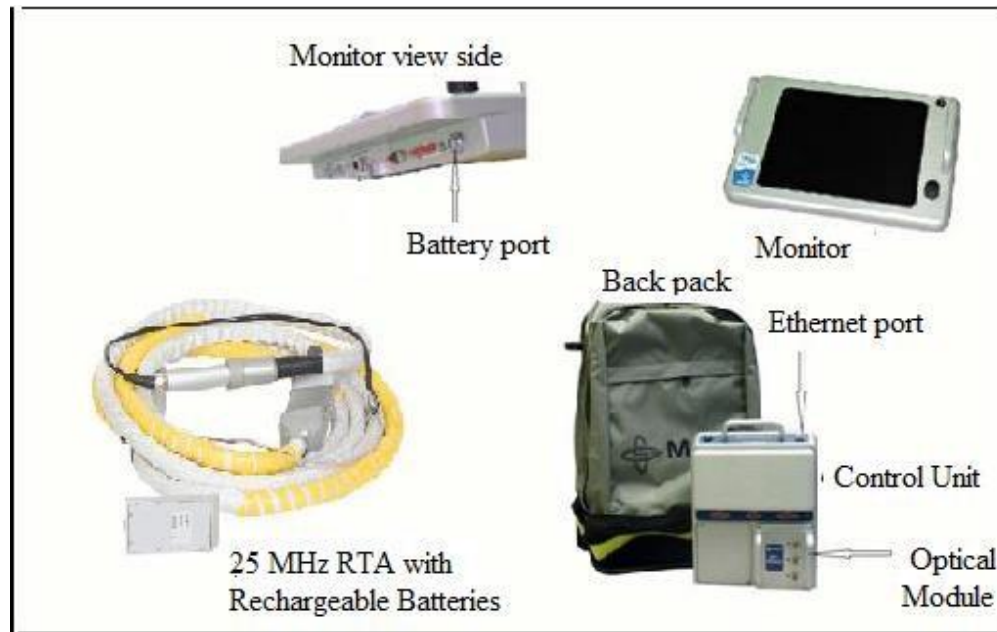
Figure: 3.4 Picture of the MALA ProEx system and its various components (MALA Geoscience, 2003).

3.3.2.2 GPR Data Acquisition using Mala ProEx System

During the field data survey, 25 MHz rough terrain antenna was employed in collecting the data. The survey was carried out along five profiles with lengths ranging from 80 m to 200 m.The unshielded rough terrain antenna, as well as the rest of the device, were setup and the backpacked positioned at the back of the field personnel. The setup was then configured by entering the necessary acquisition parameters, such as the antenna type, data acquisition mode, velocity etc. The setup was then towed (Fig. 3.5) along the profile for the data acquisition.

A)   (B)

Figure: 3.5 Showing (A, B) a project student carrying out GPR survey at the project site

The main components of the ground penetration radar system are shown in the figure 3.6. The system enables the transmitter (Tx) to generate a wave train of radio waves, which propagates within a broad beam. When the wave train comes across an obstacle, the wave train is either reflected or refracted back to the receiving antenna (Rx). As the antenna is moved over the ground, the signals are displayed as a function of two-way travel time in the form of a radargram.
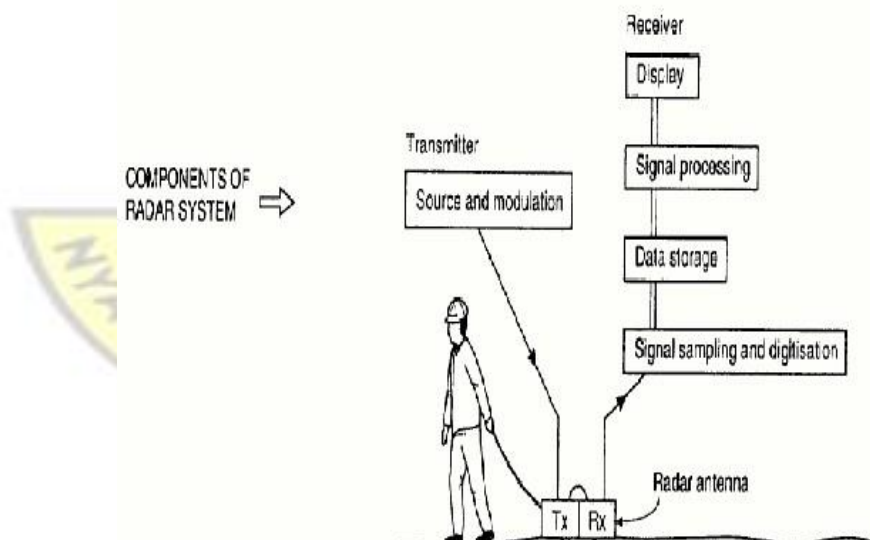
Figure: 3.6 Schematic diagram showing how GPR system under operation. (MALA Geoscience, 2003).

3.3.2.3 Processing of GPR data using REFLEXW

The various data collected from the field were imported and converted using the

REFLEXW software. The data sets were processed using various filters such as, Dewow

(subtract - mean), the static correction, the time gain, the background removal and finally

the topography correction (Cassidy, 2009). Dewowing (subtract-mean) was the first filter

employed in removing obscure images or low frequency components of the data from the

ground penetration radar survey. This helped to reduce the data to a mean zero position

(Annan, 2005). This process also helped to compensate for the delayed time of the early

arrivals of the waves or the wriggles and helped to improve the visual quality of the data

(Cassidy, 2009).

3.3.2.4 Static Correction:

In the ground penetration radar survey, the waveforms, which first arrived at the point of

the receiver is the air waves, within the radar area. Hence the static correction stage was

carried out, to correct and compensate for any static errors. In this process the traces were

readjusted to common time zero point. During static correction, the waves were enhanced.

This helps to improve the resolution of the images. In this case, the realignment causes all

reflections beneath to be correctly aligned (Cassidy, 2009).

3.3.2.5 Time Gain

The time gain filter was employed to compensate for any possible amplitude variation due

to attenuation within the ground penetration data. During processing, the reflections from

the deeper depth are observed to be greater than that of the near subsurface reflections, due

to the geometric spreading, as well as the intrinsic attenuation. This helps in adjusting the

38

lapse time, as the wavelet proceed to die out. Hence, the time gain process helped to increase the signal to noise ratio, as well as enhancing the resolution of the arrivals of the waves, that appears later, as a result of signal attenuation and geometrical spreading losses (Cassidy, 2009).

3.3.2.6 Topographic correction

In order to carry out the topography correction, the respective elevations recorded along the individual profile lines were imported into the processing data package, so that the travel time of each elevation point will be computed. The data is then adjusted to positive time, as the correction is applied to each of the trace. The results of the data, reflected the state of the individual topography along the profile. This process aided in revealing the correct position and orientation of geologic features such as folding; cavities faulting, bedrocks and hydro-geologic features, such as water tables. Furthermore, these features can be clearly seen, from the pseudo-sections generated from the subsurface earth.

3.3.2.7 Some challenges encounter during the GPR Surveying

Among the difficulties uncounted during the GPR survey, were some environmental problems such as improper mining or harvesting of clay at the site. This has led to the ponds of water in most points in the area. The improper mining makes (figure 3.7 and figure 3.8) it impossible to have straight profile in some areas within the project site. As a result, there were some offsetting along some profiles to make it possible to cover full length of the planned profiling**.**

(A)   **(B)**

Figure: 3.7 (A, B) Shows a pictorial views of an improper mining of clay at the project site

The profile along which the resistivity and GPR survey were conducted are shown in figure 3.8.
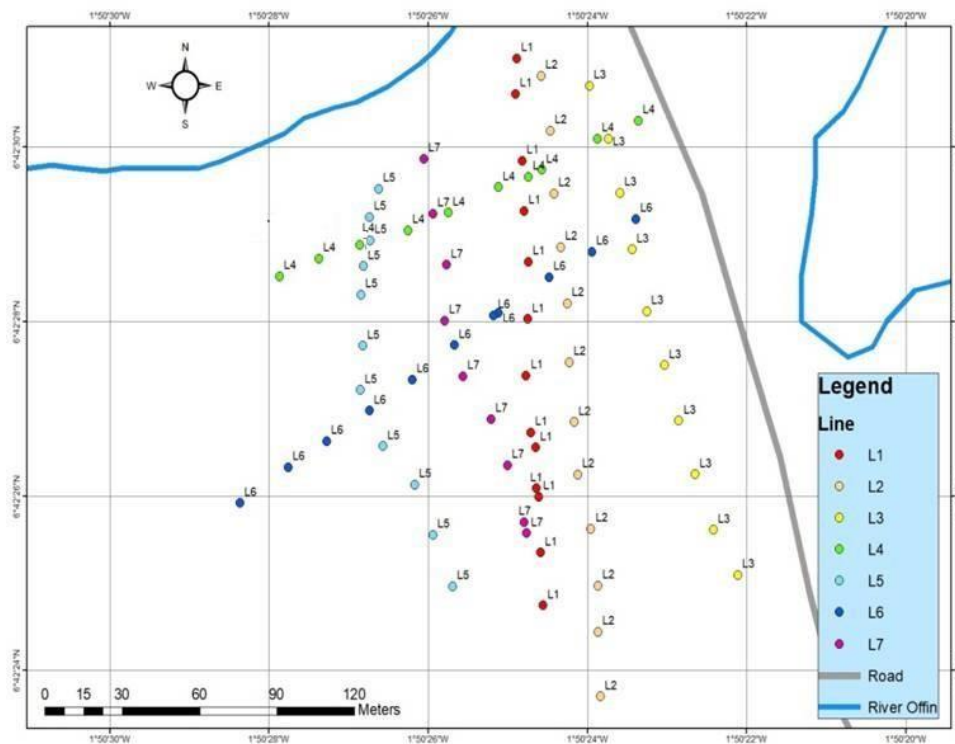
Figure: 3.8 Source: Showing a generated map of the project area, indicating the various sampling points (Source: ArcGIS, 2013, Version 10.6)

3.3.3 Particle Size Distribution Analyses

3.8.8 Materials and Equipment used for the Particle Size Distribution test

The materials used for the gradation test include: weighing balance, cleaning brush, blender, timing device, 152 hydrometer, sedimentation cylinder, set of sieves (British standard (BS), sieve shaker, stirrer and control cylinder as shown in figure 3.9.
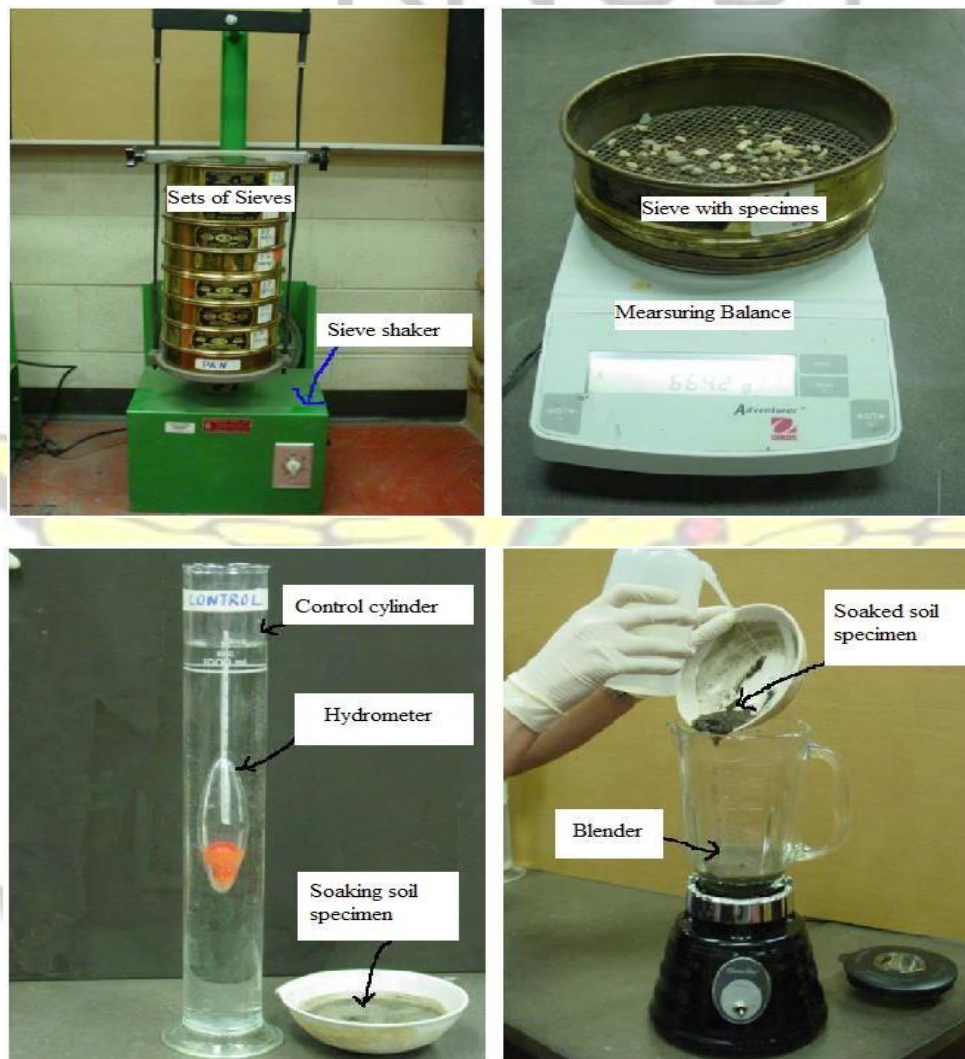
Figure: 3.9 some equipment used for the particle size distribution analyses test (Source: Google search)

3.3.3.1 Procedure for the Gradation Analyses

Five samples were collected at different part of the site and the location coordinates recorded using GPS. The particle size distribution analysis was determined using the ASTMD 422 – Standard of soil testing (i.e. American society of testing and material Division). This enables the determination of the particle size distribution of the random soil specimen collected at the project site. The test was carried out at the Civil Engineering laboratory, at the Kwame Nkrumah University of Science and Technology, Kumasi.

3.3.3.2 Steps for the Sample Preparation for Wet Sieving

The samples were passed through a riffle box and weigh between (500-1000) gm. The weighed sample is then sieved through British standard (BS) test sieve 2.00 mm. The fraction less than 2.00 mm diameter was blended, poured into a rubber bowl and flooded with water for 24 hours. The soaked samples were washed and dried in an oven for at least 16hours.

3.3.3.2 Procedure

The BS test sieves were selected and arranged in the order (2.00, 3.18, 4.75, 6.70, 9.50, 13.20, 19.00, 26.5, 37.1, 53.00, 63.0, 75.00) mm for samples less than 75 mm. For sample ranging between 0.75 to 2.00 mm the sieves were arranged as (0.075, 0.100, 0.200, 0.300, 0.425, 0.600, 1.00) mm. The samples were separated into various fractions by sieving through the various sieves in descending order. The weight of soil retained on each sieve was weighed and recorded.

CHAPTER FOUR

RESULTS AND DISCUSSION

4.1 Introduction

This Chapter discusses the detailed description of the resistivity pseudo-sections as a reflection of the variations of the lithostratigraphy along the profile. Also, there was a display of ground penetration radar along some of the selected profiles taken in the study site. These helped in the mapping of the depths to the bed rock and water table. Similarly, noticeable reflections revealed on the different portions of the radargram were used in the estimation of the subsurface structures in the area. Grain size distribution analysis results that helped in characterization of the subsurface materials were also discussed.

4.2 Geophysical Characterization

Geophysical characterization of the subsurface deposit most often involves, the measurement of the physical properties of subsurface materials. This result is then interpreted to determine the thickness and the lateral extent, depth to bedrock,hence the thickness of the overburden materials.Also determined from these results were the water table within the area.

4.3 Electrical Resistivity Results

4.3.1 Electrical Resistivity Tomography of Profile 1

Figure 4.1 is the electrical resistivity tomography of profile L 1. It can be observed from this image that, at the near subsurface (depth range of 0 to 5 m) of the profile, two main distinct resistivity zones can be identified. The low resistive zone with resistivity value less than 20 Ωm labelled 'C' (between 25 to 35 m and 125 to 141 m of the profile length) were considered to be clay rich zones saturated with water. The second zone with

moderatelyhigh resistivity values (115-200 Ωm) on the remaining portion of the profile. This second layer is considered to comprise mainly of sandy clay. The high resistive signature at the beginning of the profile which is located very close to the bank of the river can be attributed to the washed up sand from the river. Further beneath these layers lie relatively uniform geologic zone with resistivity value around 200 Ωm at a depth range of 5 to 17.5 m. This zone is seen to have extension of the low resistivity zone at the beginning and the midportions of the profiling. This low resistive material, may be attributed to the extension of the clayey layer or the infiltration of water from the water saturated clayey surface layer.

The moderately-high apparent resistive (115-588 Ωm) within this zone can be attributed to the increase in gravel/silt soil, from the weathered granitic rock. Below this zone is the zones of very high resistivity labelled BRK with resistivity value greater than 1329 Ωm. This zone is considered to be the granitic bedrock with different degree of alteration.
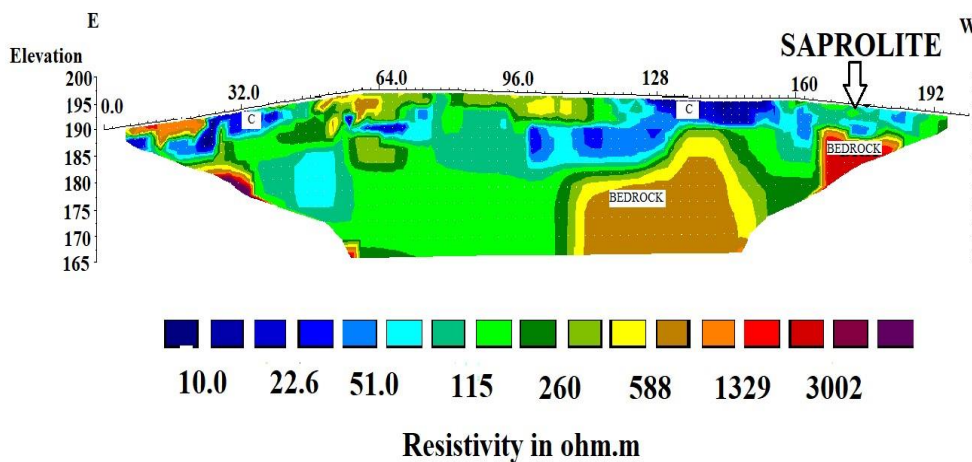
Figure 4.1: 2D Resistivity Distribution of profile L 1.

4.3.2 Electrical Resistivity Tomography of Profile L 2

The electrical resistivity tomography (ERT) of profile two (figure 4.2), gives an information of the geologic formations in the area. The resistivity value range of 10 to 588Ωm in the near surface (depth up to 5 m), as one traversed laterally along the profile. The very low resistivity zones labelled C, which were considered to be position of clay layer is observed from 130 to 195 m along the profile length. Below this layer is moderately high resistivity zone (115 to 500 Ωm), that extends laterally along the profiling from the near surface to a depth of 32.2 m, from 0 to 128 m of the profile length, which can be attributed to sandy soil. Whiles that of the moderately, low resistivity materials may be attributed to a weathered or saturated soil, such as clayey silt soils from the weathered granite. The most highly resistivity zone labelled BRK, may be attributed to the granitic bedrock.
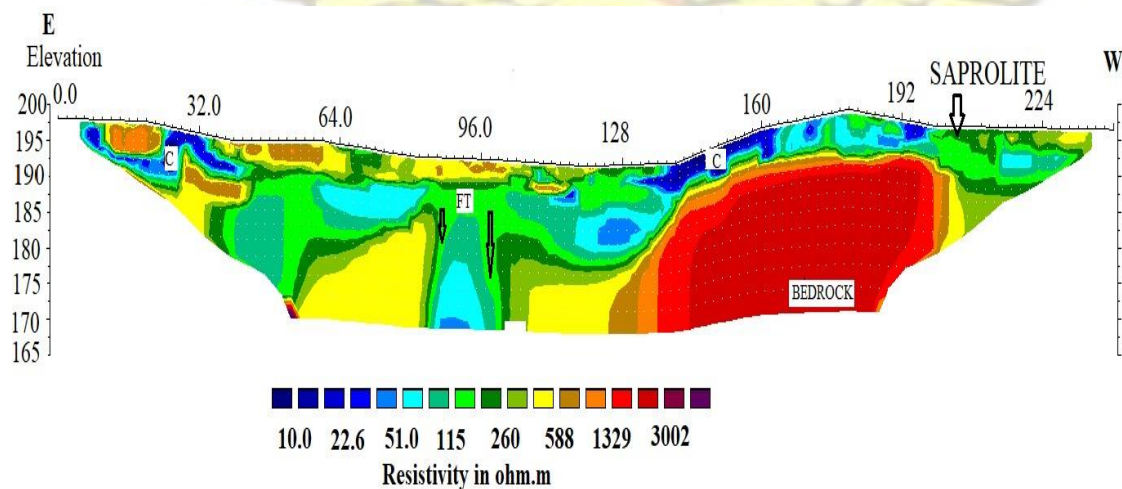
Figure 4.2: 2D Resistivity Distribution of profile L 2.

4.3.3 Electrical Resistivity Tomography of Profile L 3

The resistivity section of profile three (figure 4.3) also produced three distinct resistivity zones. Laterally along the surface, the high resistivity sandy layer extends across most parts along the profiling. Similarly, the relatively low to moderately resistive clayey soils, embedded within the beginning and close to the ends of the profiling. The high resistive layer observed at an elevation range of 192.5-172.5 m, may be attributed to sandy soil, with less moisture content. This profile which is along the river channel shows the extent of the averagely 5 m thick sandy soil at the bank of the river. Below this layer is the saprolite layer, as well as the deep bottom layer, considered to be the bedrock (BRK).

Figure 4.3:2D Resistivity Distribution of profile L 3

4.3.4 Electrical Resistivity Tomography of Profile L 4

The profile line four (figure 4.4), the near surface high resistive anomaly, extends from 64 m to the end of the profile length, at a depth of approximately 15m. The low resistivity zone as observed in previous section is attributed to the possible conductive materials, or water saturated body. The low resistivity zones considered to be clay rich layer, at an elevation range of 195 to 185 and depth of 10 m beneath subsurface. The medium to high resistive zone ($\geq 200\Omega$m) be this layer could be attributed to both sandy/silt to

46

sandy/gravelly soils and the resistive signatures of the impermeable granitic bed rock, at a depth 32.5m, with an elevation range of 197.5 to 165 m beneath the earth surface.
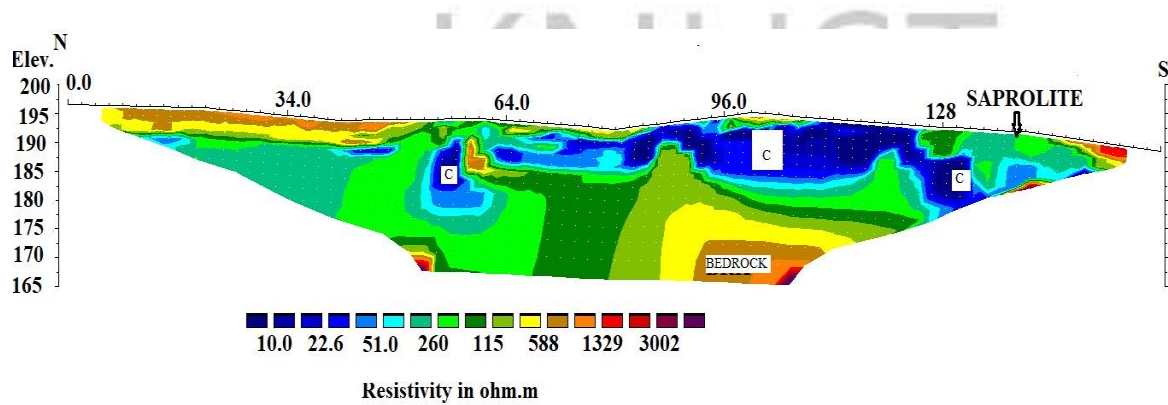
Figure 4.4: 2-D Resistivity Distribution of profile 4.

4.3.5 Electrical Resistivity Tomography of Profile L5

Profile five (Figure 4.5) gives an indications of a low resistivity anomaly (100Ωm) zone at the near surface, with some patches of medium resistive geologic materials. The low resistivity layer is observed from 0 to 128 m length of the profile. The depth/thickness extent of this layer is 5 m but extends to a depth/thickness of 10 m between elevations of 185 to 175 m. This layer could be attributed to a saturated soil such as clayey/silt soil layers, or water formation. The high resistive anomalies layers may also be attributed to a gravellysandy soil, as well as the impermeable granitic bedrock. With a depth of 20 within an elevation of 180 to 160 m beneath near surface.
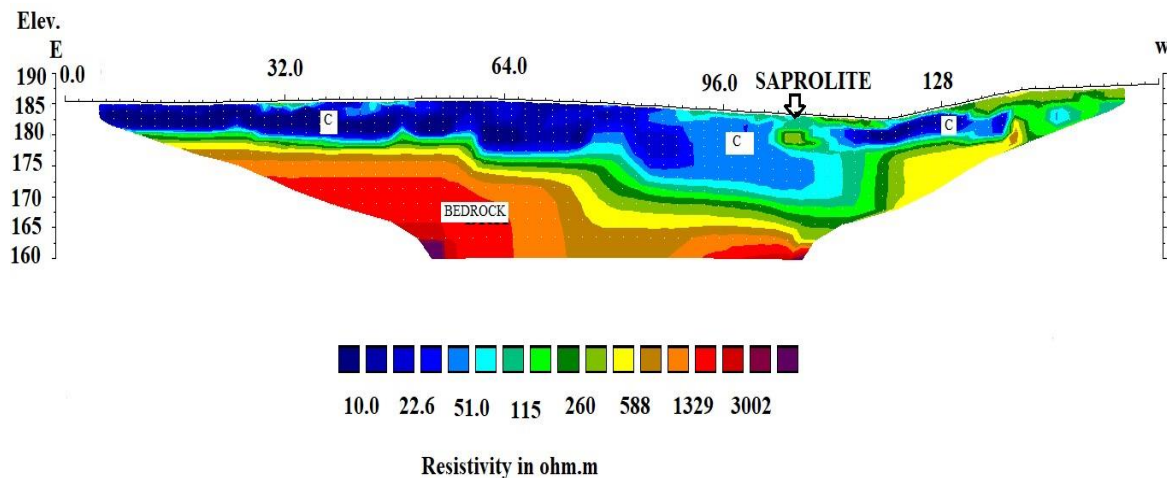
Figure 4.5: 2 – D Resistivity Distribution of profile L 5

4.3.6 Electrical Resistivity Tomography of Profile L 6:

From this profile (figure 4.6), a moderate high resistivity zone at the near surface (250 to 588 Ωm) which extends to a depth of 5m was observed from the beginning to 96 m of the profiling length. Also observed is the low resistivity zone 'C' which is attributed to a high saturated geologic layer such as silt/clayey soil, with thickness of 15m, within an elevation of (195 to180) m. The underlying materials, with highly resistive values, could be due to the presence of unweathered granitic saprolite, and the presence of the sandy/gravelly depositions., at a depth of 25 m, beneath the earth subsurface.
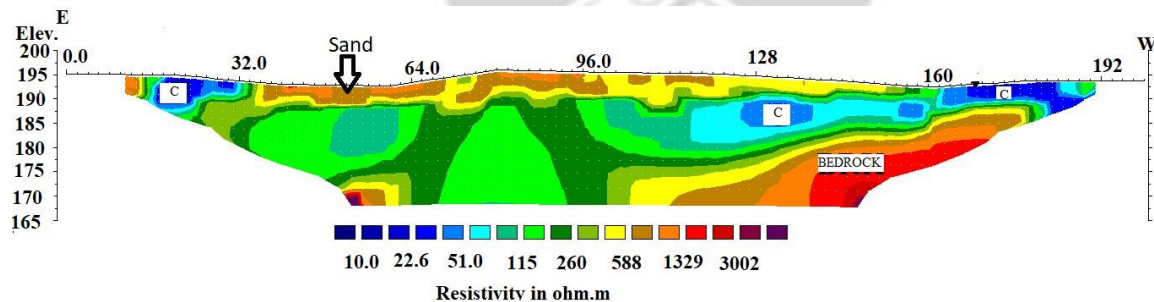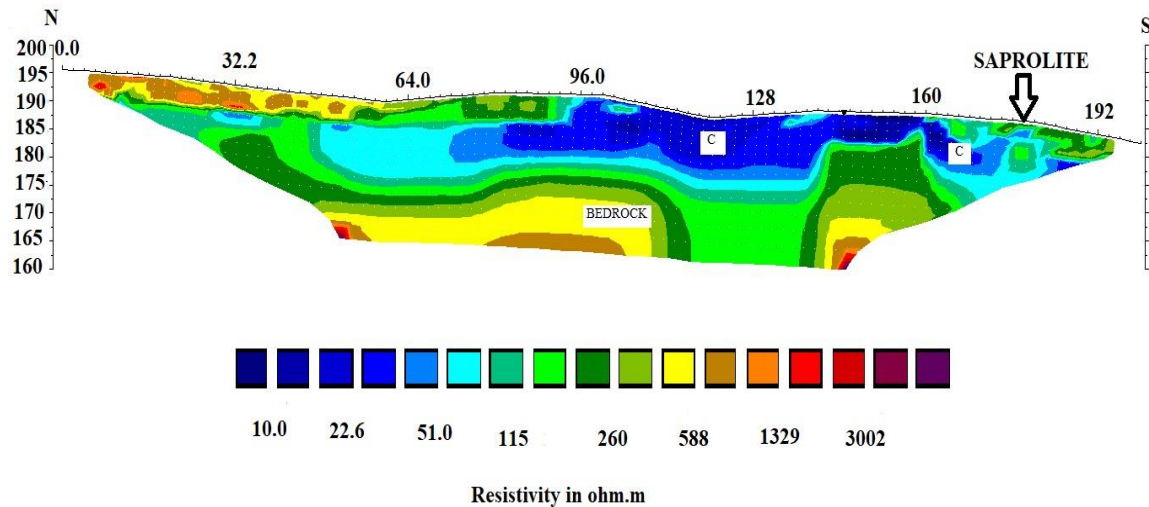
Figure 4.6: 2-D Resistivity Distribution of profile L 6.

4.3.7 Electrical Resistivity Tomography of Profile L 7

This profile (Figure 4.7) shows mostly low resistivity anomalies, with moderately resistive patched anomalies along the whole length of the profile. The very low resistivity zone extends, from the subsurface through to the possible fractured structure/layer, labelled (FT) was worth noted in this image (Figure 4.7). This could be attributed to a fracture zone or the infiltration of water from excavated clay pit at the site. Again the high resistive zones of deposition can be attributed to the sandy/gravel(100-260 Ωm) materials, as well as the impermeable ($\leq$ 588 Ωm) granitic bedrock.
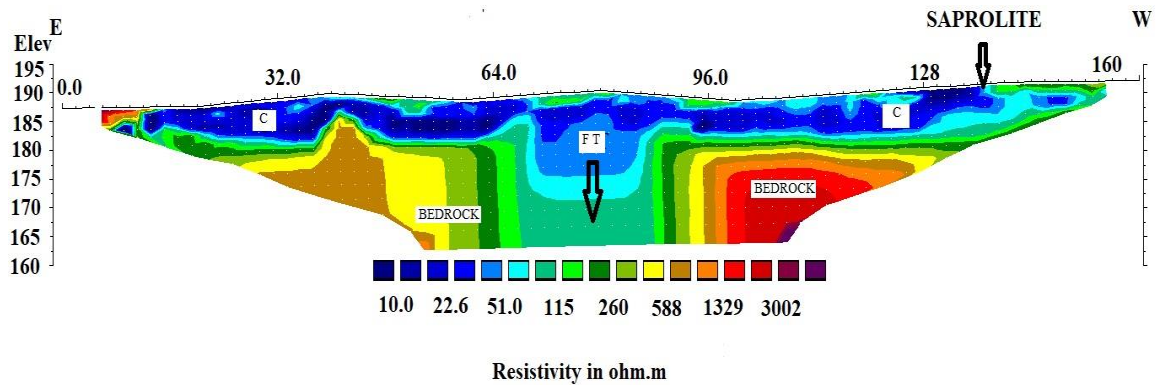
Figure 4.7: 2D Resistivity Distributions for profile 7

4.4 GPR RESULTS

4.4.1 Introduction

The application of the GPR radargram in the lithostratigraphic characterization of the subsurface lithological units depends on the contrast of the dielectric properties of the subsurface materials. The reflections occur as a result of changes in the bulk dielectric permittivity. These changes can be attributed to change in grain size, density (porosity), lithology, and saturation. This produces different reflection patterns which can be used to map the volume of the deposition, the thickness of the overburden, as well as the depth to water table. Furthermore, this method can be used in the discrimination and the mapping of different geological medium. Generally, geological boundaries and water table produce continuous horizontal reflections (Milsom, 2007) with formation of some lithological unit producing coherent reflection (Reynolds, 2011). The oblique reflections are produced at interfaces made up of sandy layers of different grain size or sand and clay sediments (Reynolds, 2011).

4.4.2 RADARGRAM SECTIONS

The GPR survey was carried out on five profiles using a rough terrain antenna of frequency 50 MHz, producing a GPR radargram sections with maximum depth of 60 m. From the analysis of the radargram sections (figure 4.8A to 4.8D), three distinct lithological zones can be distinguished. The radargrams of most of the profiles show a smooth reflection pattern attributed to weathered saprolitic layers. On profiles one, three, and four, (figure 4.8A, 4.8C and 4.8D), the first two zones (F1 and F2) can be distinguished. The thickness range of layerF1 is between 5 to 10 m, which is shown as a smooth reflection pattern. This is considered to be produced by a finer grain soil sample (clay). The second zone F2 seem, closely gritty in appearance at depth of 10 m was attributed to an increasing grain size with depth. This is considered to be made of weathered granitic rock (saprolite). The strong oblique reflections labelled 'R' as observed in the radargrams in these zones are produced at the interface between sandy layers (Reynold, 2011) and the clay layer as mapped in the resistivity sections (figures 4.1 to 4.7). Below this zone is the third zone considered to be the bedrock. The boundary between this zone and the weathered saprolitic layers are marked with a distinct horizontal line (Milsom, 2007). The relatively homogeneous radargram produced in this layer may be attributed to coarsely geologic formation with low conductive surface such as granitic rock due to its less moisture content.

Profile two, (fig.4.9) produces an extension of the saprolitic layer as a sharp break in the radar reflections between 75m to125m at a depth of 15m.This may be as a result of the conductive nature of the water saturated clayey/silt soil or a fracture in the area. The final profile line (fig. 4.5E) shows relatively homogeneity radargram from the beginning to the ends of the profile. Also observed in the upper layers in the radargram figure 4.8C is

another horizontal reflection surface considered to be the water table shown with horizontal

arrows.
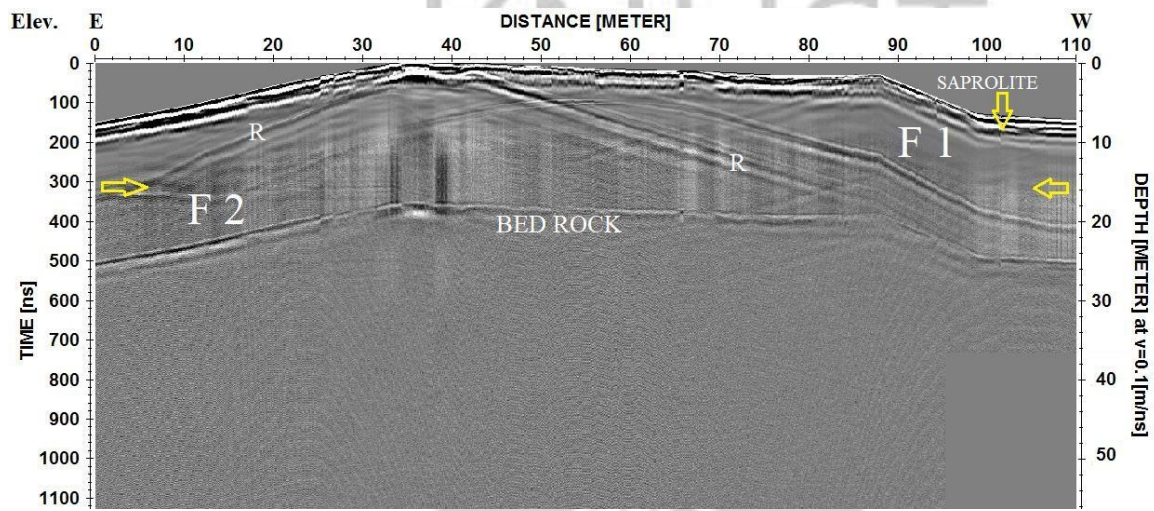
Figure 4.8A: Radargram of profile   L 1
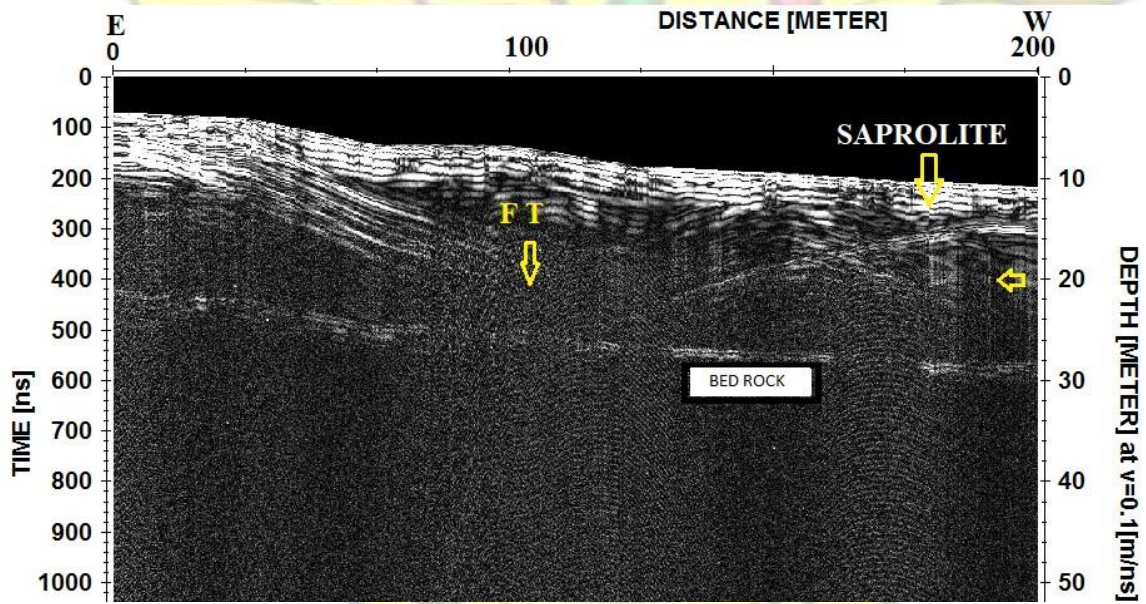
Figure 4.8B: Radargram of profile L 2
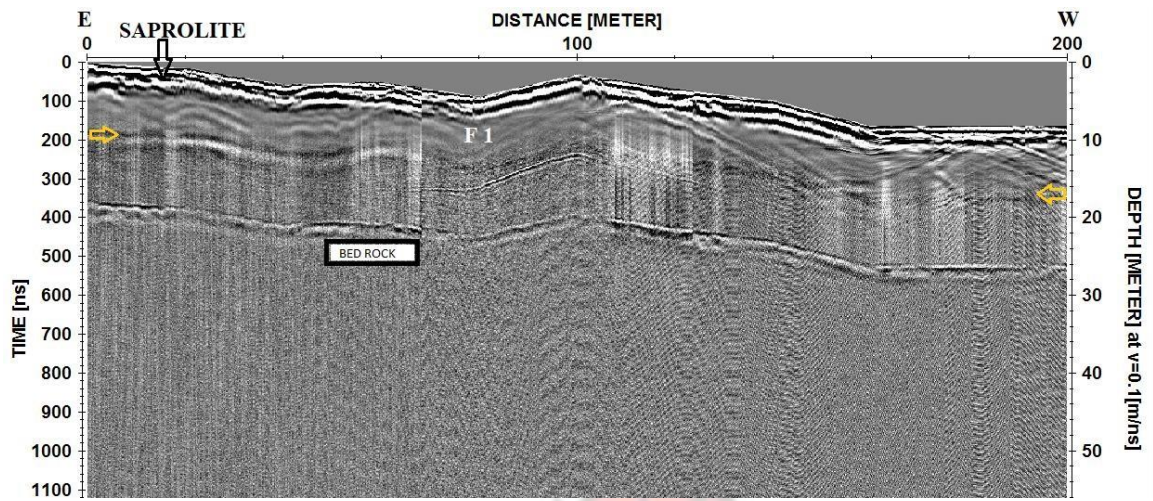
Figure: 4.8C: Radargram of profile L 3
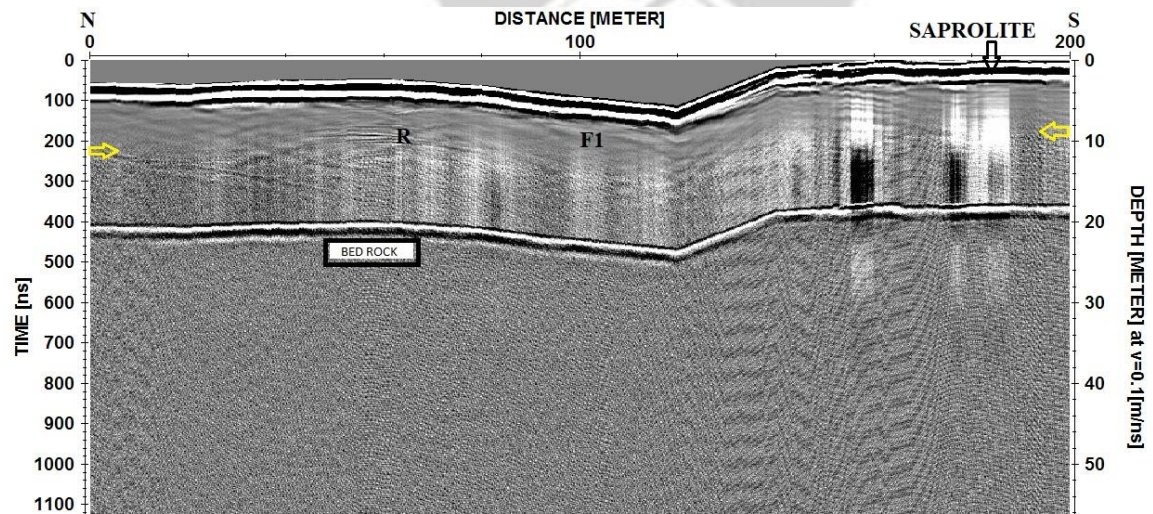
Figure 4.8D: Radargram of profile L 4
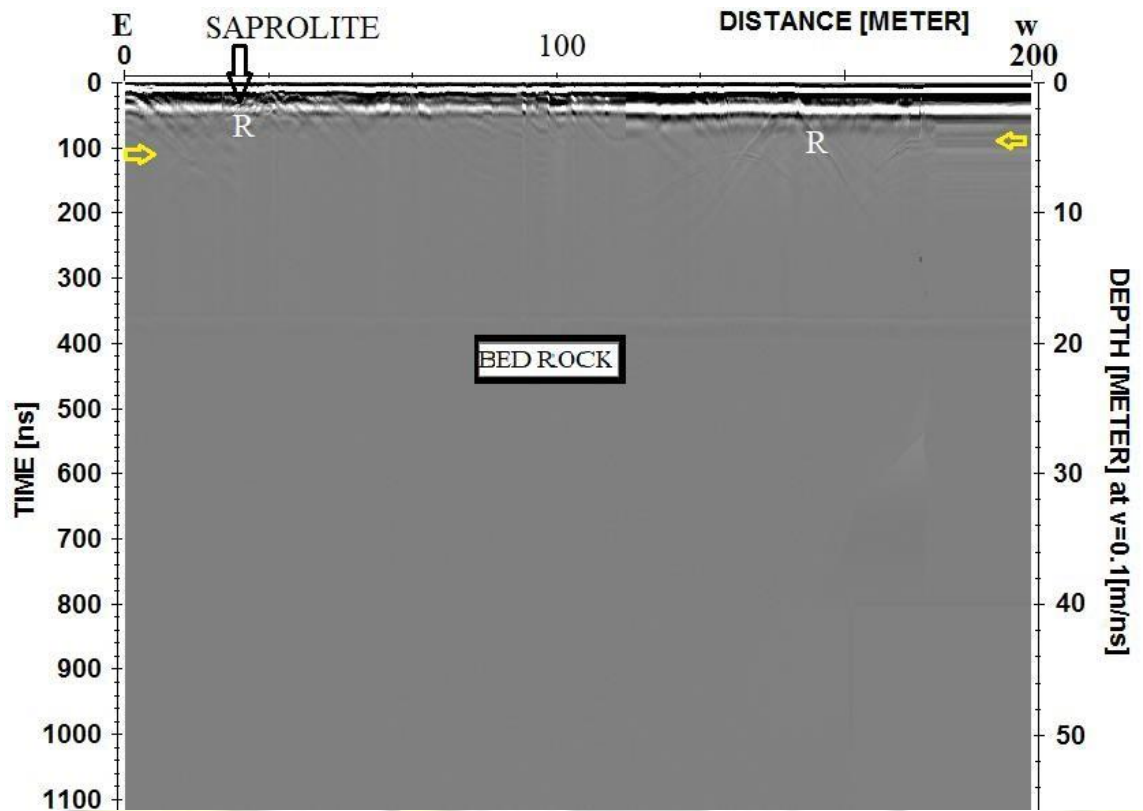
Figure 4.8E: Radargram of profile L 5

4.5 Quantitative Analyses of the Particle Size Distribution Test.

4.5.1 Soil Sample 1

The grain size analysis diagram of sample 1 (figure 4.10) reveals four (4) different soil types. The sample had about five percent (5%) of the samples passing between sieve diameter ranges of 0.00 – < 0.002 mm. From the grading curve, the silt zones, were also seen to have thirty per cent (30%) passing within a sieve diameter of 0.002 -0.06mm. Furthermore, sixty-three percent (63%) passed through the sieve of diameter 0.06 – 2 mm. The gravel zones were seen to have 2 per cent (2%) passing with a sieve diameter range of 2 to 10 mm. From this result, the sandy soil was considered to be the most dominant subsurface material within the southern zone of the project site.
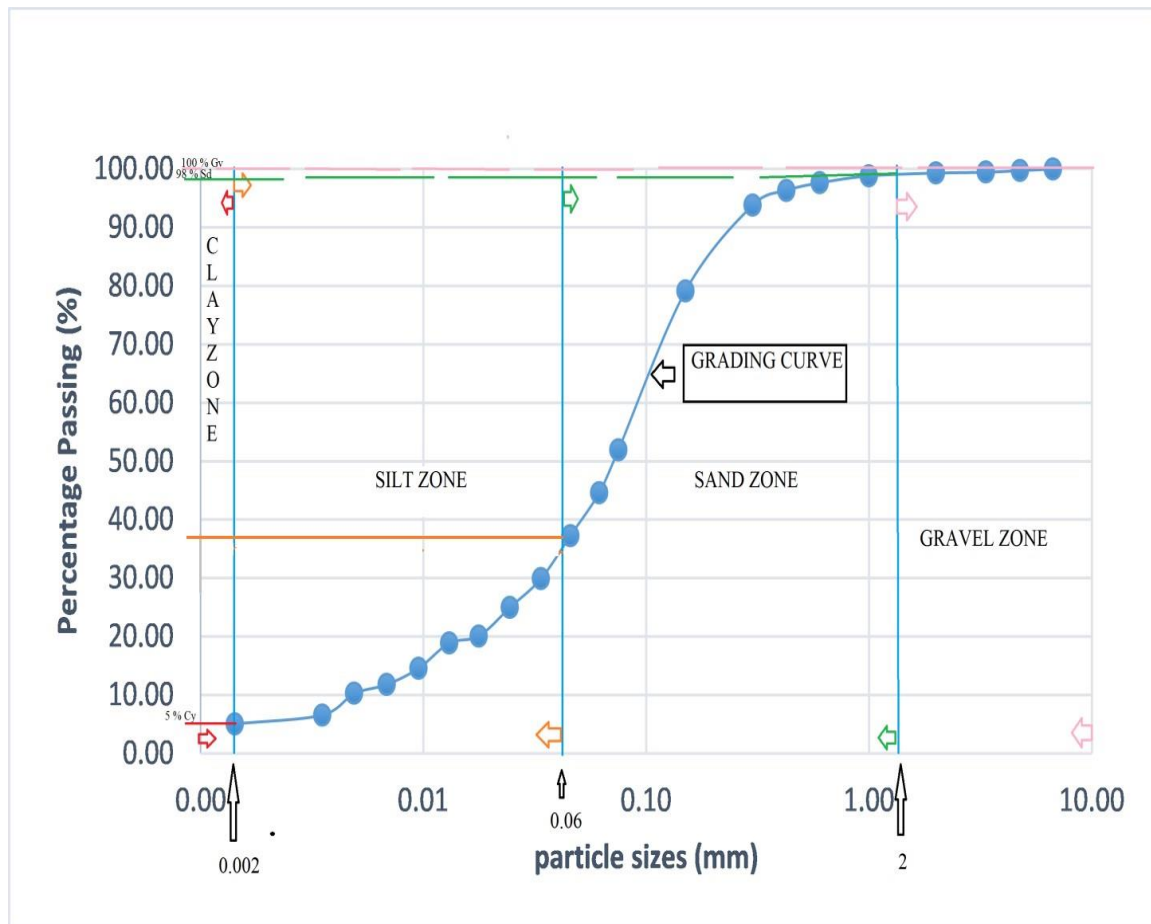
Figure 4.10: Grading curve for soil sample 1

4.5.2 Soil Sample Point 2

The sample point 2, located within the western zones of the project site, have four (4) different subsurface materials, involving, clayey, sandy, silts and gravels. Tracing from the grading curve, the clay materials, have five per cent (5%), whiles, the silts have twentythree (23%) percent of the sample passing 0.06 mm sieve diameter. Also, the sand has seventy-one (71%) per cent passing through the sieve, with the gravel having (1%) passing through the sieve of diameter 2mm respectively. Hence, in considering the sample point 2, sandy soil seems to dominate, compared to the other soil types.
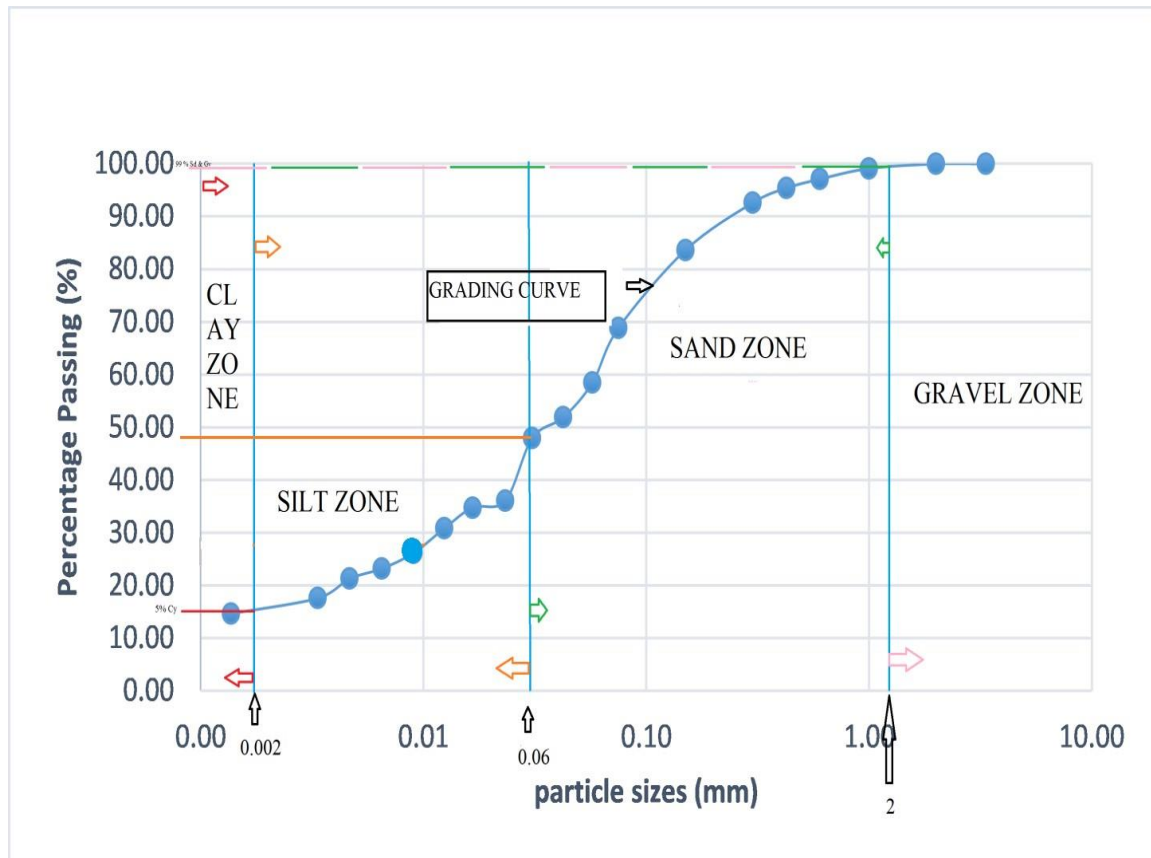
Figure 4.11: Grading curve for soil sample 2

4.5.3 Soil Sample Point 3

The grading curve (figure 4.12) for sample 3, located within the northern portions of the project site, indicates four (4) subsurface materials. The sample consist of 24% clay, 34% silts, 41% sand and 1% gravel. Hence at the sample point 3, it was noted that both sand/gravel soils, seems to have dominance among the other geologic soils present.
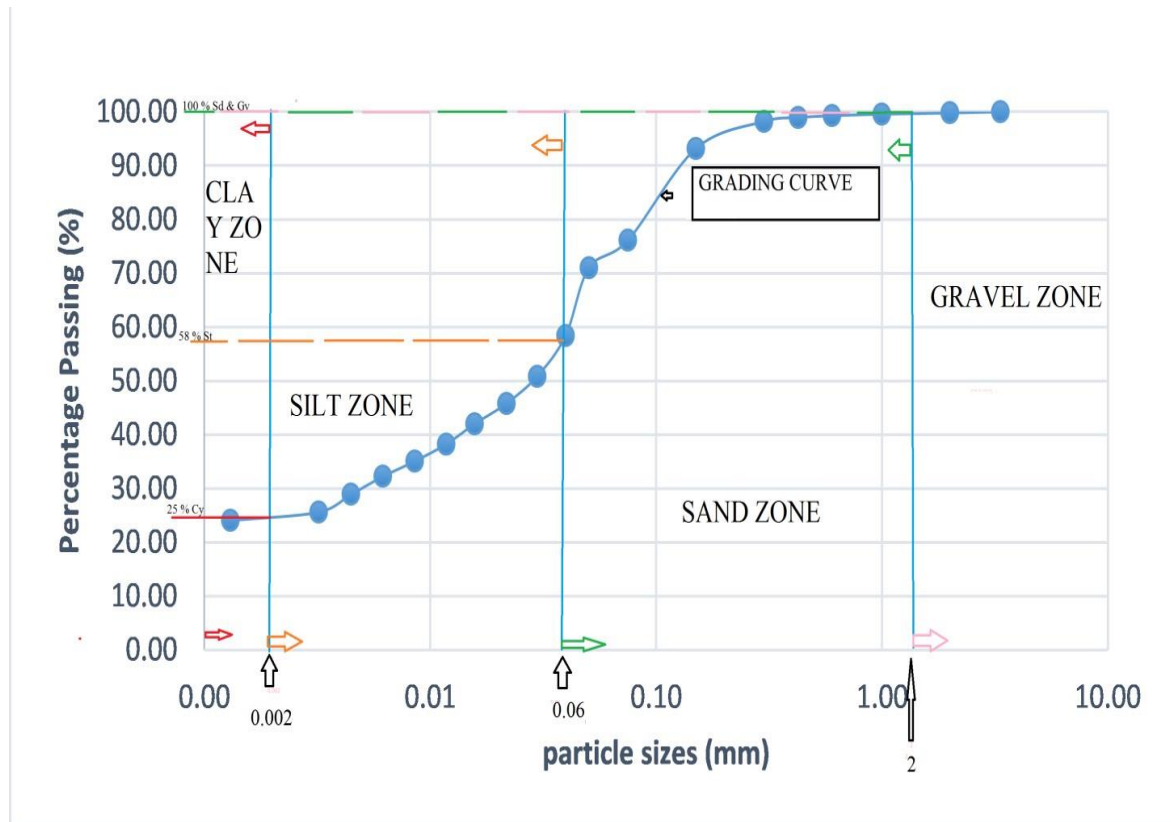
Figure 4.12: Grading curve for soil sample 3

4.5.4 Soil Sample Point 4

From the sample 4 located within the eastern side of the project site, the grading curve indicates four (4) subsurface materials. The sample consist of 2% clay, 8% silts, 86% sand and 4% gravel. This result indicates that, this area is dominated with sandy/gravel material, with little clayey or silt material.
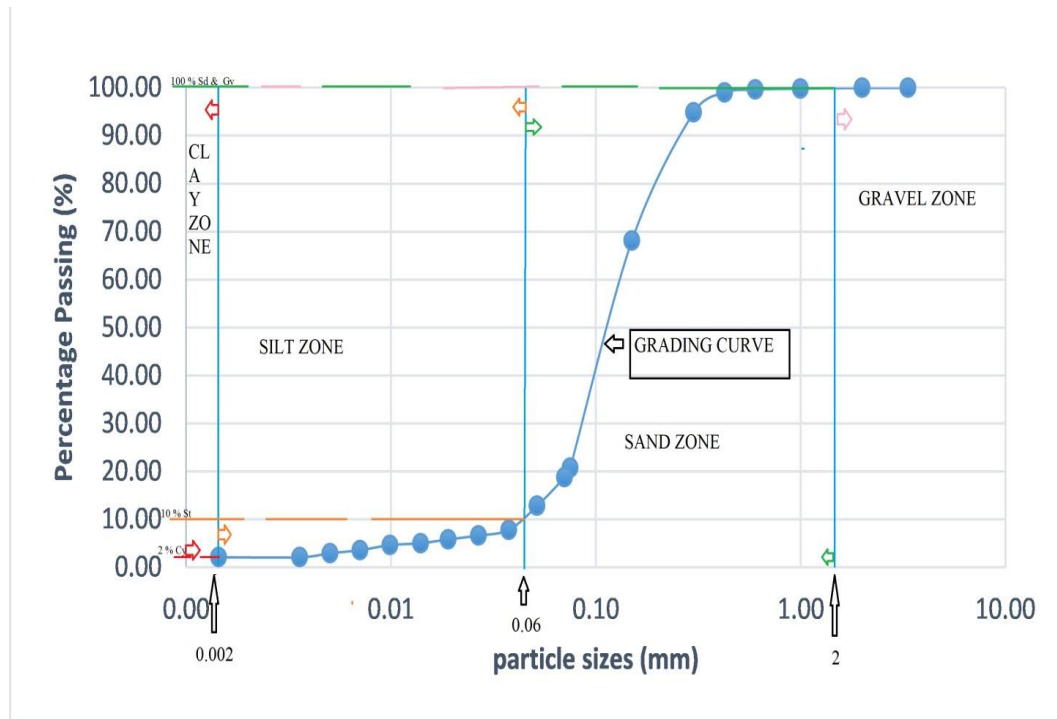
Figure 4.13 Grading curve for soil sample 4

CHAPTER FIVE

CONCLUSIONS AND RECOMMENDATIONS

5.1 Conclusion

The electrical resistivity and the ground penetration radar methods were used to map out the possible lithological units at the Kyereyiase clay deposit, in the Atwima Nwabiagya South District of the Ashanti Region. These methods, helped in delineating, the lateral extent and the thickness of the clayey soil and other lithological units. The depth to bedrock and the water table were also mapped. The result of two dimensional electrical resistivity

tomography (2D ERT) depth, gives better resolution and enhanced subsurface lithological representation of the area. From the result, the sandy clay (weathered granitoid saprolite) layer was mapped with resistivity range of 10 to 500 Ωm. The saprolitic material (Overburden layer) was found to have an average thickness of 25 m. The rich clay layer was mapped to have average thickness range of 5 to 10 m and lateral extent of 64 to 94 m. The depth to the granitoids bedrock layer was mapped to be a depth range of 20 to 30 m beneath ground surface. Furthermore, the GPR technique, helped in determining the water table within an average depth of 16 to 20 m. The particle size distribution analysis conducted on selected sediments sample from the project site showed that sediment consist of clay, silt, sand and gravel. The compositions were the range of 2 to 24% for clay, 8 to 34 % for silt, 41 to 86% for sand and 1 to 4% for gravel. These methods have proven effective in lithostratigragraphic characterization of the clay deposit site at Kyereyiase. This work can be repeated in other areas to help map and quantify the amount of clay deposit in the area.

5.2 Recommendation:

1. 3 D model of data collection must be employed, together with 2D model, in any future related survey, as this allows the user to interpret stratigraphic units in greater detail, with high resolution.

2. As the electrical techniques are not the only panacea in subsurface investigations, borehole logs and outcropping data may be required to collaborate the results of any electrical method used.

REFERENCES

Atwima Nwabiagya District Assembly Report, 2013; 2012.

Annan, A.P., 2005. Ground penetrating in near surface geophysics, Butler DK (Ed). Society of exploration geophysicists. Tulsa, investigations in Geophysics, 13; 357 – 438.

Cassidy, N.J., 2009. Ground penetrating radar data processing, modeling and analysis. In applications, Jol Hm (Ed). Elsevier: Amsterdam; 141- 176.

Banton, O., Seguin, M.K. and Cimon, M.A., 1997. Mapping field scale physical properties of soil with electrical resistivity. Soil sci., soc. Am.61: 1010-1017.

Brewster, M.L. and Annan, A.P., 1994. Ground-Penetrating radar monitoring of a controlled DNAPL release: 200MHZ radar Geophysics, 59(8): 1211-1221.

Barker, R.D., 1989. Depth of investigation of a generalized 4-electrode array: Geophysics, 54:1031-1034.

Barker, R.D., 1981.The offset system of electrical resistivity sounding and its use with a multicore cable. Geophysical prospecting 29(1):128-143.

Churchman, G.J., Gates, W.P., Theng, B.K.G. and Yuan, G., 2006. Chapter 11.1 Clays and Clay Minerals for Pollution Control". Developments in Clay Science. In: Bergaya, et al. (ed.) Handbook of Clay Science. Elsevier.1: 625–675.

Daniels, J., Ehsani, M.R. and Allerd, B., 2008.Ground-penetration radar methods (GPR). Handbook of agricultural geophysics, CRC Press, Taylor and Francis Group, Boca Raton, Florida, 129-146.

Daniels, D.J., 2004. Ground penetration Radar, 2nd Edition. The institution of electrical engineers. London, England, 726p.

Daniels, J.D., 1996.Surface penetrating radar. Electronics and communication Engineering journal, 8(4):165-182.

Davis, J. and Annan, A., 1989. Ground penetrating radar for high-resolution mapping of soil and rock stratigraphy 1. Geophysical prospecting, 37(5):531-551.

Eisenlohr, B. and Hirdes, W., 1992.The structural development of the early Proterozoic Birimian and Tarkwaian rocks of Southwest Ghana West Africa journal of African East Sciences,14 (3):313-325.

Fokkema, J.T., Fokkema, E., Beekman, S. and Slob, E.C., 2001. Analysis of georadar reflection responses. In: 7th International congress of the Brazilian Geophysical Society, Salvador-Bahia.

Gazoty, A., Fiandaca, G., Pedersen, E., Auken, E., Christiansen, A.V. and Pedersen, J.K., 2012. Application of time domain induced polarization to the mapping of litho types in a landfill site. Hydrol. Earth Syst. Science 16, 1793-1804.

Ghana statistical Service, 2012.Population and housing census (PHD) Report, Ghana Statistical Service, Accra.

Ghana statistical Service, 2010. Population and housing census (PHD) Report, Ghana Statistical Service, Accra.

Holtz, W.G., 1948. The determination of limits for the control of placement moisture in high rolled-earth dams. Proc. Amer. Sot. civ. Engrs, 48: 1240-1248.

Huggenberger, P., 1993.Radar facies: recognition of facies patterns and heterogeneities within Pleistocene Rhine gravels, NE Switzerland. Geological society, London, special publications, 75(1): 163-176.

Habberjam, G.M., 1979. Apparent resistivity observations and the use of square array techniques, Vol. 9, Balogh Scientific Books.

Jol, H.M. and Bristow, C.S., 2003. GPR in sediments: advice on data collection, basic processing and interpretation, a good practice guide in ground penetration radar in sediments. Geological Society: London, special publication, 211: 9-28.

Junner. N., 1935. Gold in gold coast. Accra, Ghana: Geological Survey Department.

Kearey. P., Brookes, M. and Hill, S., 2002. An introduction to Geophysical exploration. Black well science.
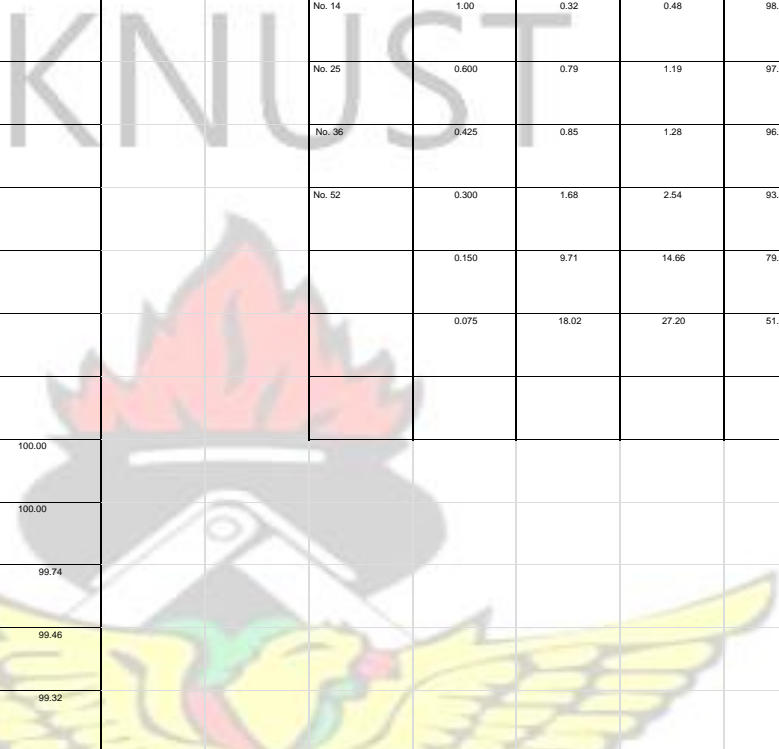
Kesse, G.O., 1985. The mineral and rock resources of Ghana, United States. .A .Balkema publishers.

Loke, M.H., 2012. Tutorial: 2D and 3D electrical imaging surveys. Penang, Malaysia, University stains Malaysia.

Loke, M.H., 2001. Tutorial: 2D and 3D electrical imaging surveys. Penang, Malaysia, University stains Malaysia. Unpublished course note, http://www.geoelectrical.com.

Loke, M., 1999. Electrical imaging surveys for environmental and engineering studies.

Loke, M.H. and Barker, R.D., 1996. Rapid least-squares inversion of apparent resistivity pseudo sections by a quasi-Newton method. Geophysical prospecting, 44(1):131152.

Leube, A., Hirdes, W., Mauer, R., and Kesse, G.O., 1990. The early Proterozoic Birimian Supergroup of Ghana and aspect of its associated gold mineralization. Precambrian Research, 46(1-2):139-165.

Leube, H.A. and Hirdes, W., 1986. The Birimian Supergroup of Ghana depositional environment, Structural development and Conceptual model of an Early Proterozoic suite. Rept No 99529, Arch. BGR: 260p, Hannover (Unpubl.)

Merriman, R.J., 2006. Clay Minerals and Sedimentary Basin History. European Journal of Mineralogy, 17(1): 7-20.

MALA GeoScience, Inc., 2003. Introductory Training Course Manual. For RAMAC/GPR.

Milsom, J., 2007.Field Geophysics, volume 25.John Wiley and sons Ltd, New York.

Preko, K. and Wilhelm, H., 2012. Detection of water content in homogeneities in a dike model using invasive GPR guided wave sounding and TRIME- TDR technique. Journal of Geophysics and Engineering, 9(3):312-329.

Preko, K., 2007. Volumetric soil water determination, using ground penetrating radar (GPR).PHD thesis, Geophysical institute, university of Karlsushe.

Reynolds, J.M.. 2011. An introduction to applied and environmental geophysics. John Wiley and Sons.

Reynolds, J.M., 1997. An introduction to applied and environmental geophysics. John Wiley and Sons. Chichester, England, 796.

.Sucre, E.B., Tuttle, W. and Fox, T.R., 2010. The use of ground-penetration radar to accurately soil depth in rocky forest soils. Forest Science 57: 59-66.

Scollar, I., Tabbagh, A., Hesse, A. and Herzog, I., 1990. Archaeological prospecting and remote sensing. Cambridge University Press.

Schmutz, M., Revil, A., Vaudelet, P., Batzle, M., Viñao, P.F. and Werkema, D.D., 2010. Influence of oil saturation upon spectral induced polarization of oil-bearing sands. Geophysical Journal International 183, 211-224.

Telford, W.M., Geldart L.P. and Sheriff, R.E., 1990. Applied Geophysics. Cambridge university press, second edition.

Telford, W.M., Geldart, L. P. and Sheriff, R.E., 1976. Applied Geophysics. Cambridge: Cambridge university press, Cambridge.

Tsiboah, T. and Grant, T., 2009. Application of Geophysics to Gold Exploration in Ghana: Examples from Newmont Projects ASEG Conference.

Weems, J.B., 1904. Chemistry of Clays". Iowa Geological Survey Annual Report, 14(1): 319–346. doi:10.17077/2160-5270.1076. ISSN 2160-5270.

Wemegah, D.D., Fiandaca, G., Auken, E., Menyeh, A. and Danuor, S. K., 2017. Spectral time-domain induced polarisation and magnetic surveying − an efficient tool for characterisation of solid waste deposits in developing countries. EAGE Near Surface Geophysics, 15(1), 75-84.DOI: 10.3997/1873-0604.2016048.

APPENDIX 1:

Soil sample results for: Particle size distribution analysis Analyses

Sample ID:- No 390										
GRADING TEST	Weight (g)	66.2								66.24

Sieve size		Weight	Percentage	Percentage			Sieve size		Weight	Percentage	Percentage
BS designation (ins)	Metric	retained	retained	passing			BS designation (ins)	Metric	retained	retained	passing
	(mm)	(g)	(%)	(%)				(mm)	(g)	(%)	(%)
2.953	75.00						No. 14	1.00	0.32	0.48	98.84
2.480	63.00						No. 25	0.600	0.79	1.19	97.64
2.087	53.00						No. 36	0.425	0.85	1.28	96.36
1.461	37.10						No. 52	0.300	1.68	2.54	93.83
1.043	26.50							0.150	9.71	14.66	79.17
0.748	19.00							0.075	18.02	27.20	51.96
0.520	13.20										
0.374	9.50			100.00							
0.264	6.70		0.0	100.00							
0.187	4.75	0.17	0.3	99.74							
0.132	3.35	0.19	0.3	99.46							
0.079	2.00	0.09	0.1	99.32							

Hydrometer readings

Elapsed time,(min)	Time (mins)	Temp (° c)	Direct hydrometer readings Rh'	Reading Rh'	Rh=Rh' + Cm	Hr (mm)	Viscosity	D (mm)	Temp Corr.Mt	Rd= Rh'Ro'+Mt	K (%)
0.50	7:50	28.00	1.0200	20.00	20.5	119.6250	0.8279	0.0615	1.7861	18.1861	44.61
1.00	7:51	28.00	1.0170	17.00	17.5	131.4750	0.8279	0.0456	1.7861	15.1861	37.25
2.00	7:52	28.00	1.0140	14.00	14.5	143.3250	0.8279	0.0337	1.7861	12.1861	29.89
4.00	7:54	28.00	1.0120	12.00	12.5	151.2250	0.8279	0.0245	1.7861	10.1861	24.99
8.00	7:58	28.00	1.0100	10.00	10.5	159.1250	0.8279	0.0177	1.7861	8.1861	20.08
15.00	8:05	28.00	1.0095	9.50	10.0	161.1000	0.8279	0.0130	1.7861	7.6861	18.86
30.00	8:20	27.00	1.0080	8.00	8.5	167.0250	0.8472	0.0095	1.5249	5.9249	14.54
60.00	8:50	26.50	1.0070	7.00	7.5	170.9750	0.8571	0.0068	1.3984	4.7984	11.77
120.00	9:50	26.00	1.0065	6.50	7.0	172.9500	0.8672	0.0049	1.2745	4.1745	10.24
240.00	11:50	26.00	1.0050	5.00	5.5	178.8750	0.8672	0.0035	1.2745	2.6745	6.56
1440.00	7:50	27.50	1.0040	4.00	4.5	182.8250	0.8375	0.0014	1.6542	2.0542	5.04

Sample ID:- No391

GRADING TEST		Weight (g)		68.0							68.01
Sieve size		Weight	Percentage	Percentage			Sieve size		Weight	Percentage	Percentage
BS designation	Metric	retained	retained	passing			BS designation (ins)	Metric	retained	retained	passing

Sieve size	(mm)	(g)	(%)	(%)			Sieve size	(mm)	(g)	(%)	(%)
2.953	75.00						No. 14	1.00	0.04	0.06	99.94
2.480	63.00						No. 25	0.600	0.08	0.12	99.82
2.087	53.00						No. 36	0.425	0.12	0.18	99.65
1.461	37.10						No. 52	0.300	0.15	0.22	99.43
1.043	26.50							0.150	0.74	1.09	98.34
0.748	19.00							0.075	2.32	3.41	94.93
0.520	13.20										
0.374	9.50										
0.264	6.70										
0.187	4.75										
0.132	3.35			100.00							
0.079	2.00		0.0	100.00							

Hydrometer readings

Elapsed tme,(min)	Time (mins)	Temp (° c)	Direct hydrometer readings Rh'	Reading Rh'	Rh=Rh' + Cm	Hr (mm)	Viscosity	D (mm)	Temp Corr,Mt	Rd= Rh'Ro'+Mt	K (%)
0.50	7:50	28.00	1.0370	37.00	37.5	52.4750	0.8279	0.0408	1.7861	35.1861	84.07
1.00	7:51	28.00	1.0355	35.50	36.0	58.4000	0.8279	0.0304	1.7861	33.6861	80.49
2.00	7:52	28.00	1.0340	34.00	34.5	64.3250	0.8279	0.0226	1.7861	32.1861	76.90
4.00	7:54	28.00	1.0320	32.00	32.5	72.2250	0.8279	0.0169	1.7861	30.1861	72.13
8.00	7:58	28.00	1.0305	30.50	31.0	78.1500	0.8279	0.0124	1.7861	28.6861	68.54
15.00	8:05	28.00	1.0285	28.50	29.0	86.0500	0.8279	0.0095	1.7861	26.6861	63.76
30.00	8:20	27.00	1.0270	27.00	27.5	91.9750	0.8472	0.0070	1.5249	24.9249	59.55
60.00	8:50	26.50	1.0245	24.50	25.0	101.8500	0.8571	0.0053	1.3984	22.2984	53.28
120.00	9:50	26.00	1.0225	22.50	23.0	109.7500	0.8672	0.0039	1.2745	20.1745	48.20
240.00	11:50	26.00	1.0195	19.50	20.0	121.6000	0.8672	0.0029	1.2745	17.1745	41.04
1440.00	7:50	27.50	1.0175	17.50	18.0	129.5000	0.8375	0.0012	1.6542	15.5542	37.16

Sample ID:- No 393

GRADING TEST	Weight (g)		64.5								64.49
Sieve size		Weight	Percentage	Percentage			Sieve size		Weight	Percentage	Percentage
BS designation (ins)	Metric	retained	retained	passing			BS designation (ins)	Metric	retained	retained	passing
	(mm)	(g)	(%)	(%)				(mm)	(g)	(%)	(%)
2.953	75.00						No. 14	1.00	0.15	0.23	99.55
2.480	63.00						No. 25	0.600	0.18	0.28	99.27

Sieve size							Sieve size		Weight	Percentage	Percentage
2.087	53.00						No. 36	0.425	0.22	0.34	98.93
1.461	37.10						No. 52	0.300	0.47	0.73	98.20
1.043	26.50							0.150	3.24	5.02	93.18
0.748	19.00							0.075	11.00	17.06	76.12
0.520	13.20										
0.374	9.50										
0.264	6.70										
0.187	4.75										
0.132	3.35			100.00							
0.079	2.00	0.14	0.2	99.78							

Hydrometer readings

Elapsed time,(min)	Time (mins)	Temp (° c)	Direct hydrometer readings Rh'	Reading Rh'	Rh=Rh' + Cm	Hr (mm)	Viscosity	D (mm)	Temp Corr.Mt	Rd= Rh'Ro'+Mt	K (%)
0.50	7:50	28.00	1.0300	30.00	30.5	80.1250	0.8279	0.0504	1.7861	28.1861	71.02
1.00	7:51	28.00	1.0250	25.00	25.5	99.8750	0.8279	0.0398	1.7861	23.1861	58.42
2.00	7:52	28.00	1.0220	22.00	22.5	111.7250	0.8279	0.0297	1.7861	20.1861	50.86
4.00	7:54	28.00	1.0200	20.00	20.5	119.6250	0.8279	0.0218	1.7861	18.1861	45.82
8.00	7:58	28.00	1.0185	18.50	19.0	125.5500	0.8279	0.0158	1.7861	16.6861	42.05
15.00	8:05	28.00	1.0170	17.00	17.5	131.4750	0.8279	0.0118	1.7861	15.1861	38.27
30.00	8:20	27.00	1.0160	16.00	16.5	135.4250	0.8472	0.0086	1.5249	13.9249	35.09
60.00	8:50	26.50	1.0150	15.00	15.5	139.3750	0.8571	0.0062	1.3984	12.7984	32.25
120.00	9:50	26.00	1.0138	13.80	14.3	144.1150	0.8672	0.0045	1.2745	11.4745	28.91
240.00	11:50	26.00	1.0125	12.50	13.0	149.2500	0.8672	0.0032	1.2745	10.1745	25.64
1440.00	7:50	27.50	1.0115	11.50	12.0	153.2000	0.8375	0.0013	1.6542	9.5542	24.07

Sample ID:- No394

GRADING TEST Weight (g)   61.6   61.64

Sieve size		Weight	Percentage	Percentage			Sieve size		Weight	Percentage	Percentage
BS designation	Metric	retained	retained	passing			BS designation (ins)	Metric	retained	retained	passing
	(mm)	(g)	(%)	(%)				(mm)	(g)	(%)	(%)
2.953	75.00						No. 14	1.00	0.53	0.86	99.11
2.480	63.00						No. 25	0.600	1.25	2.03	97.08
2.087	53.00						No. 36	0.425	1.05	1.70	95.38
1.461	37.10						No. 52	0.300	1.72	2.79	92.59
1.043	26.50							0.150	5.52	8.96	83.63
0.748	19.00							0.075	9.12	14.80	68.84

0.520	13.20			
0.374	9.50			
0.264	6.70			
0.187	4.75			
0.132	3.35			100.00
0.079	2.00	0.02	0.0	99.97

Hydrometer readings

Elapsed tme,(min)	Time (mins)	Temp (° c)	Direct hydrometer readings Rh'	Reading Rh'	Rh=Rh' + Cm	Hr (mm)	Viscosity	D (mm)	Temp Corr,Mt	Rd= Rh'Ro'+Mt	K (%)
0.50	7:50	28.00	1.0240	24.00	24.5	103.8250	0.8279	0.0573	1.7861	22.1861	58.49
1.00	7:51	28.00	1.0215	21.50	22.0	113.7000	0.8279	0.0424	1.7861	19.6861	51.90
2.00	7:52	28.00	1.0200	20.00	20.5	119.6250	0.8279	0.0308	1.7861	18.1861	47.94
4.00	7:54	28.00	1.0155	15.50	16.0	137.4000	0.8279	0.0233	1.7861	13.6861	36.08
8.00	7:58	28.00	1.0150	15.00	15.5	139.3750	0.8279	0.0166	1.7861	13.1861	34.76
15.00	8:05	28.00	1.0135	13.50	14.0	145.3000	0.8279	0.0124	1.7861	11.6861	30.81
30.00	8:20	27.00	1.0120	12.00	12.5	151.2250	0.8472	0.0090	1.5249	9.9249	26.16
60.00	8:50	26.50	1.0110	11.00	11.5	155.1750	0.8571	0.0065	1.3984	8.7984	23.19
120.00	9:50	26.00	1.0104	10.40	10.9	157.5450	0.8672	0.0047	1.2745	8.0745	21.29
240.00	11:50	26.00	1.0090	9.00	9.5	163.0750	0.8672	0.0034	1.2745	6.6745	17.60
1440.00	7:50	27.50	1.0075	7.50	8.0	169.0000	0.8375	0.0014	1.6542	5.5542	14.64

Sample ID:- No 395

GRADING TEST Weight (g) 81.5 81.46

Sieve size		Weight	Percentage	Percentage			Sieve size		Weight	Percentage	Percentage
BS designation (ins)	Metric	retained	retained	passing			BS designation (ins)	Metric	retained	retained	passing
	(mm)	(g)	(%)	(%)				(mm)	(g)	(%)	(%)
2.953	75.00						No. 14	1.00	0.11	0.14	99.83
2.480	63.00						No. 25	0.600	0.17	0.21	99.62
2.087	53.00						No. 36	0.425	0.50	0.61	99.01
1.461	37.10						No. 52	0.300	3.41	4.19	94.82
1.043	26.50							0.150	21.75	26.70	68.12
0.748	19.00							0.075	38.55	47.32	20.80

0.520	13.20			
0.374	9.50			
0.264	6.70			
0.187	4.75			
0.132	3.35		100.00	
0.079	2.00	0.03	0.04	99.96

Hydrometer readings

| Elapsed tme,(min)	Time (mins)	Temp (º c)	Direct hydrometer readings Rh'	Reading Rh'	Rh=Rh' + Cm	Hr (mm)	Viscosity	D (mm)	Temp Corr,Mt	Rd= Rh'Ro'+Mt	K (%)
0.50	7:50	27.00	1.0115	11.50	12.0	153.2000	0.8472	0.0705	1.5249	9.4249	18.80
1.00	7:51	27.00	1.0085	8.50	9.0	165.0500	0.8472	0.0517	1.5249	6.4249	12.82
2.00	7:52	27.00	1.0060	6.00	6.5	174.9250	0.8472	0.0376	1.5249	3.9249	7.83
4.00	7:54	27.00	1.0054	5.40	5.9	177.2950	0.8472	0.0268	1.5249	3.3249	6.63
8.00	7:58	27.00	1.0050	5.00	5.5	178.8750	0.8472	0.0190	1.5249	2.9249	5.83
15.00	8:05	27.00	1.0046	4.60	5.1	180.4550	0.8472	0.0140	1.5249	2.5249	5.04
30.00	8:20	27.00	1.0044	4.40	4.9	181.2450	0.8472	0.0099	1.5249	2.3249	4.64
60.00	8:50	26.50	1.0040	4.00	4.5	182.8250	0.8571	0.0071	1.3984	1.7984	3.59
120.00	9:50	26.00	1.0038	3.80	4.3	183.6150	0.8672	0.0050	1.2745	1.4745	2.94
240.00	11:50	25.50	1.0035	3.50	4.0	184.8000	0.8775	0.0036	1.1533	1.0533	2.10
1440.00	7:50	27.50	1.0030	3.00	3.5	186.7750	0.8375	0.0014	1.6542	1.0542	2.10

SOFTWARE USED

- Res2dinv
- ReflexW
- Source: ArcGIS,2013
- Google Earth, 2018
- Microsoft Excel

A generated satellite images of the Kyereyiase project site indicating both the sampling distribution points and the settlements.

(Source: Google Earth, 2018)
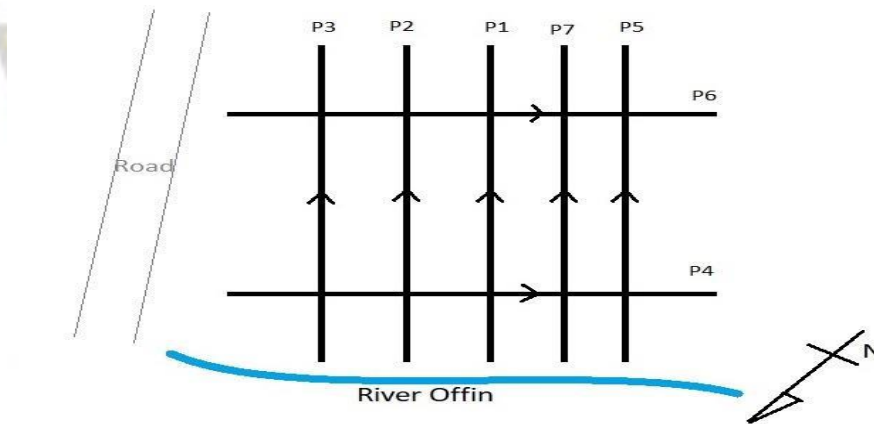
Schematic diagram, representing the profile line at the project site